Comparison Of ICA Morphometry Between Patients With Moyamoya Disease And Controls

Submitted for Post Doctoral Fellowship, Cerebrovascular Surgery
by

Dr. SANJAY HM
January 1st- December 31st, 2022

DEPARTMENT OF NEUROSURGERY

SREE CHITRA TIRUNAL INSTITUTE FOR MEDICAL

SCIENCES &TECHNOLOGY

THIRUVANANTHAPURAM – 695011

Comparison Of ICA Morphometry Between Patients With Moyamoya Disease And Controls



Submitted by : Dr. SANJAY HM

Programme : Post Doctoral Fellowship, Cerebrovascular Surgery

Month & year of submission : December, 2022

DECLARATION

This thesis titled **— Comparison Of ICA Morphometry Between Patients With Moyamoya Disease And Controls** is a consolidated report based on a bonafide study of the period from May 1st to October 31st, 2022, done by me under the Department of Neurosurgery, Sree Chitra Tirunal Institute for Medical Sciences & Technology, Thiruvananthapuram. This thesis is submitted to SCTIMST in partial fulfilment of rules and regulations of Post Doctoral Fellowship programme.

Dr. Sanjay HM
Department of Neurosurgery,
SCTIMST, Thiruvananthapuram.

CERTIFICATE

This is to certify that the thesis entitled — **Comparison Of ICA Morphometry Between Patients With Moyamoya Disease And Controls** is a bonafide work of Dr Sanjay H.M and was conducted in the Department of Neurosurgery, Sree Chitra Tirunal Institute for Medical Sciences and Technology, Thiruvananthapuram (SCTIMST), under my guidance and supervision.

Dr B Jayanand Sudhir
Additional Professor
Department of Neurosurgery,
SCTIMST,
Thiruvananthapuram

Dr. B JAYANAND SUDHIR
Additional Professor
Department of Neurosurgery
Sree Chitra Tirunal Institute for
Medical Sciences and Technology
Trivandrum
Reg. No 29147

Dr. Easwer HV,
Professor and Head of Department,
Department of Neurosurgery,
SCTIMST,
Thiruvananthapuram

Dr. EASWER H.V.
Professor & Head
Dept. of Neurosurgery
SCTIMST, Thiruvananthapuram

ACKNOWLEDGEMENT

The guidance of Dr Easwer H.V, Professor and Head of the Department of Neurosurgery, has been invaluable and I am extremely grateful and indebted for his contributions and suggestions, which were of invaluable help during the entire work. He will always be a constant source of inspiration to me.

I owe a deep sense of gratitude to Additional Prof. Dr. B Jayanand Sudhir, for the conception of the idea for this project, for his invaluable advice, encouragement and guidance, without which this work would not have been possible. His critical remarks, suggestions, helped me in achieving a high standard of work. His liaison with the engineers and technologists paved way for the use of computer softwares and hardware that made this work possible.

I am deeply indebted to Dr. Krishnakumar K, Dr. George Vilanilam, Dr. Prakash Nair, Dr. Ganesh Divakar and Dr Tobin George and I thank them for their constant encouragement, timely guidance and support. I thank my colleagues for their cooperation and help.

I am also thankful to Mr Manjunath N for helping me in the technical aspects of the study. His contribution in timely segmentation of ICAs from TOF images and central line plotting was crucial for the fruition of the task we set out to achieve. His contribution is truly the centre block of this entire project.

I thank the advisors from the Department of Imaging sciences and Intervention Radiology Dr Jayadevan ER and Dr Santhosh Kumar K whose guidance in methodology was invaluable during the initial planning for this project.

I owe a deep sense of gratitude to all the patients without whom this work would not have been possible. Through them we seek validation for our purpose in life.

I am very grateful to my father Mr Murali HG and my mother Mrs. Kannika S for the love and blessings they have showered upon me. Who I am and what I do is a product of their efforts and dreams for me. I am thankful to my sister Ms Deepthi HM for her constant

encouragement and moral support, particularly at times when the task ahead seems unsurmountable.

Dr. Sanjay HM

INDEX

INTRODUCTION	8
AIMS AND OBJECTIVES	9
REVIEW OF LITERATURE	10
MATERIALS AND METHODOLOGY	16
RESULT ANALYSIS	28
DISCUSSION	34
CONCLUSION	41
LIMITATIONS	42
REFERENCES	43
ANNEXURES	
1. Proforma	46
2. Plagiarism check	47
3. IEC approval	49

INTRODUCTION :

Moyamoya disease is a fairly rare, non atherosclerotic ischemic disease characterized by chronic progressive intracranial terminal ICA narrowing with opening up of collaterals from lenticulostriate arteries resulting in the characteristic puff of smoke appearance on angiography. The stenosis commonly extends to the proximal MCA and ACA and rarely to PCA and basilar artery (1),(2).

The disease has a bimodal age distribution, predominantly affecting children in the first decade and another peak is seen in adults later on in life (3),(4),(5). It is the most common cause of pediatric strokes in Japan. (1)

A systematic review by B.J. Sudhir et al proposed a mechanobiological hypothesis on the pathogenesis of moyamoya disease (MMD) (6). It was observed that in MMD patients, there was a loss of tortuosity in ICA measured in terms of cavernous supraclinoid angle of ICA(7),(8). It is believed that the higher cavernous supraclinoid ICA angle exerted a higher hemodynamic stress at ICA bifurcation. This higher wall shear stress could theoretically lead to vessel wall remodelling and narrowing as in MMD. (9),(10)

Kim T et al (8) found shorter distance measured from carotid canal to the carotid siphon in addition to higher cavernous-supraclinoid ICA angles.

Inter-carotid distance (ICD) has not been measured in patients with MMD. Sawant N et al (11) measured ICD in pediatric patients with no skull base pathology and found the narrowest ICD was at the level of the proximal dural ring measuring 13.4 mm. Altered growth kinetics in MMD patients may affect tortuosity and ICD.

The outcome of this study is expected to give further credence to the mechano-biological hypothesis for pathogenesis of MMD (6). It may give clarity on whether the altered morphometrics are a cause or a result of the reduced ICA blood flow in MMD. This in turn might alter the management protocols in the future.

AIM AND OBJECTIVES

Aim:

- To compare the ICA morphometric data between MMD patients and non MMD cohort

Objectives:

- To study if there's a correlation between the degree of morphometric variation and occurence of MMD.
- To compare ICA morphometric data between adults and children with MMD to assess if the morphometric variation is a result or a cause of progressive ICA narrowing.

REVIEW OF LITERATURE

Moyamoya disease is characterised by progressive stenotic occlusion of supraclinoid ICA starting at and around the ICA bifurcation(1). This results in opening of lenticulostriate collaterals across diencephalic structures causing a hazy appearance “like a puff of cigarette smoke drifting in the air” on conventional angiography, as described in 1969 by Suzuki and Takaku(12). It was first described by Takeuchi and Shimizu in 1957 as “case of hypoplasia of bilateral ICA”(13). MMD presents with ischemic features in children where as in adults it is not uncommon to see a hemorrhagic presentation (6.2% vs 1% in children)(13). Childhood strokes may be precipitated by hyperventilation, coughing, crying, etc. This is due to the resultant hypocapnea related vasoconstriction of the cerebral vasculature inducing ischemia in an already compromised circulation(14). Hemorrhage is the presentation in 40-65% adults with MMD usually in the region of basal ganglia (40%), thalamus (15%) or ventricular system (30%)(15). Hemorrhagic MMD patients were found to have a greater percentage of choroidal and thalamic anastomosis than ischemic MMD and also were of significantly higher Suzuki grading(16). Patients also can present with seizures due to areas of post infarct gliosis, focal neurological deficits, abnormal movements due to infarcts in basal ganglia region(15), and visual field defects, vertigo, ataxia etc due to involvement of posterior circulation(17). It is seen more in south east asian countries like Japan, Korea and China. However, cases are also seen in India and western countries albeit less commonly(18)(19). MMD tends to run in families and 15% cases of MMD are familial. Female are affected twice as commonly as males(13). Upto 18% cases have involvement of ICA only on one side.(20)

Moyamoya disease was graded in severity by Suzuki and Takaku in 1969 (12) as shown in table 1. The disease starts with progressive narrowing of the intracranial supraclinoid ICA bifurcation. This progressive stenosis leads to hypoperfusion leading to opening up of lenticulostriate collateral vessels. These anastamosis are broadly, 1. Network along the lateral ventricle formed by basal perforators and

cortical vessels which traverse the brain, 2. Basal collateral network formed by union of carotid and basilar perforators, 3. Surface of the brain formed by end to end anastomosis of cortical and leptomeningeal vessels and dural vessels (21). Dural extra cranial vault moyamoya vessels(13) can occur later and patients may complain of headaches..

The possible etiopathogenesis of moyamoya disease was explored through a systematic review by the co-principal investigator resulted in the postulation of a mechanobiological theory for the pathogenesis of moyamoya disease(6). In this review, six key factors i.e arterial tortuosity, vascular angles, wall shear stress, molecular factors, blood rheology and and blood vessel wall strength were implicated in the loss of balance of vascular homeostasis in MMD. A single-nucleotide polymorphism of R4810K locus in the RNF 213 gene is definitively implicated in patients with ischaemic MMD (22), where as in another locus A4399T is likely associated with hemorrhagic type of MMD (23). Moyamoya Syndrome is the occurrence of the changes in ICA in patients with known associated disorders like neurofibromatosis, sickle cell disease, down's syndrome, prior cranial radiation, Grave's disease, collagen vascular disorders, etc(21)(24). The natural history of the disease includes ischemic symptoms due to progressive ICA narrowing over a decade during which collaterals form. Once the collaterals form there is a phase of stability. (25)

Grade	Angiographic Finding
1	Narrowing of the carotid bifurcation
2	Initiation of lenticulostriate collaterals
3	Intensification of moyamoya collaterals with disappearance of MCA and ACA
4	Initiation of ECA collateral, further disappearance of supraclinoid ICA, narrowing of moyamoya collaterals, disappearance of PCA
5	Intensification of ECA collaterals, minimisation of moyamoya collateral vessels
6	Disappearance of all moyamoya collaterals. All supply derived from ECA collaterals.

DSA is believed to be the gold standard for diagnosing MMD. However, MRA has a sensitivity of 73% and a specificity of 100% in diagnosing MMD.(26)

The treatment includes direct and indirect revascularisation procedures. STA MCA bypass remains the most commonly done direct revascularisation procedure for moyamoya disease and significantly reduces risk of future strokes in both the ischemic and hemorrhagic subtypes (27) (16). Other procedures like STA ACA bypass, STA PCA bypass and occipital artery- PCA bypass are also performed(28). Indirect revascularisation take a longer time for ingrowth of vessels and to re-establish circulation in the brain. Angiogenic factors in MMD are believed to be higher in circulation and may have a role in indirect vascularisation. Indirect procedures include encephalo-myo-synangiosis (EMS), encephalo-arterio-synangiosis, encephalo-duro-synangiosis, encephalo-duro-arterio-synangiosis, encephalo-duro-arterio-myo-synangiosis (EDAMS) and encephalo-duro-galeo (periostea) synangiosis. Direct revascularisation procedure is superior to indirect procedures and should be the mainstay as the benefits outweigh the risk associated with the surgery (27) (29). In Sree Chitra Tirunal Institute of Medical Sciences and technology we perform the combined procedure. The STA is tunnelled through the base of the temporalis muscle to avoid kinking and STA MCA bypass is performed (30). The dural flap is inverted and the temporalis muscle is stitched to the margins of the durotomy completing the EDAMS procedure. Such a combined procedure is superior to indirect techniques in increasing cerebrovascular reserve capacity (31).

Anatomy and development of ICA

Vascular modelling during embryogenesis and remodelling during life is described to be part of a continuum. Anatomy influences formation of arterial pathologies, like dolicoectasia, atherosclerosis, aneurysm and MMD through it’s myriad arterial variations (32), (6). The ICA is the first intracranial artery to form on Day 24 of the growing embryo. It is formed from the third branchial arch artery’s fusion with the ipsilateral counterpart of the paired dorsal aortas. The 2nd branchial arch artery forms

the ventral pharyngeal artery which disconnects distally from dorsal aorta to form the ECA and fuses proximally with the 2nd branchial arch artery to form CCA. The ICA thus, is the sole blood supply to meet the demands of the developing primitive brain. There is a great link between demand and subsequent supply and resultant arterial remodelling, not only during development but during adult life as well. Whenever a tissue outgrows it's blood supply angiogenesis is triggered due to tissue hypoxia and there is 'mechanical sprouting', i.e. formation of capillaries. This leads to a fall in impedance that leads to change in flow hemo-dynamics and subsequent vascular remodelling. At 28 days, the ICA formed divides into anterior and posterior division. The anterior division supplies the primitive optic and olfactory regions. The posterior division develops into fetal PCA, posterior choroidal artery and superior cerebellar artery.

As the occipital lobe, brainstem and cerebellum develop the posterior circulation development gets initiated. At 4-5 mm stage of the developing embryo, there are a pair of parallel neural arteries that supply the hind brain. Distally the developing hind brain is supplied by the fetal PCA and a mesh of vessels on the surface of the developing hind brain. Proximally, there are segmental arteries i.e trigeminal, otic, hypoglossal and preatlantal arteries that carry blood from the ICA on that side to the ipsilateral paired neural artery. The paired neural arteries fuse distally to form the basilar artery at the 5-8 mm stage. The first 3 segmental arteries disappear within a week of their first appearance. At 7-12 mm stage of the growing embryo, the vertebral artery develops from the cervical intersegmental arteries fusion with the proatlantal artery. The horizontal part of the vertebral artery that meet the proximal end of the basilar artery is the incorporation of the proatlantal artery at the distal end of developing vertebral artery. The origin of the vertebral artery from the subclavian artery is at the level of the sixth cervical intersegmental artery.

At 35 days (11-12mm crown rump length of the embryo) the first MCA is seen. It is primarily plexiform, and is a major blood supply to the developing brain. At the 16-18 mm stage of the embryo, the plexiform vessels fuse to give rise to a single vessel. At 18 mm crown rump length the anterior division gives rise to ACA and this

gives rise to the ophthalmic artery. The anterior communicating artery is formed at the 21-24 mm stage (at 6-7 weeks) and around this time the fetal PCA gives rise to posterior communicating artery and the distal fetal PCA proximally connects to the basilar artery. (32)

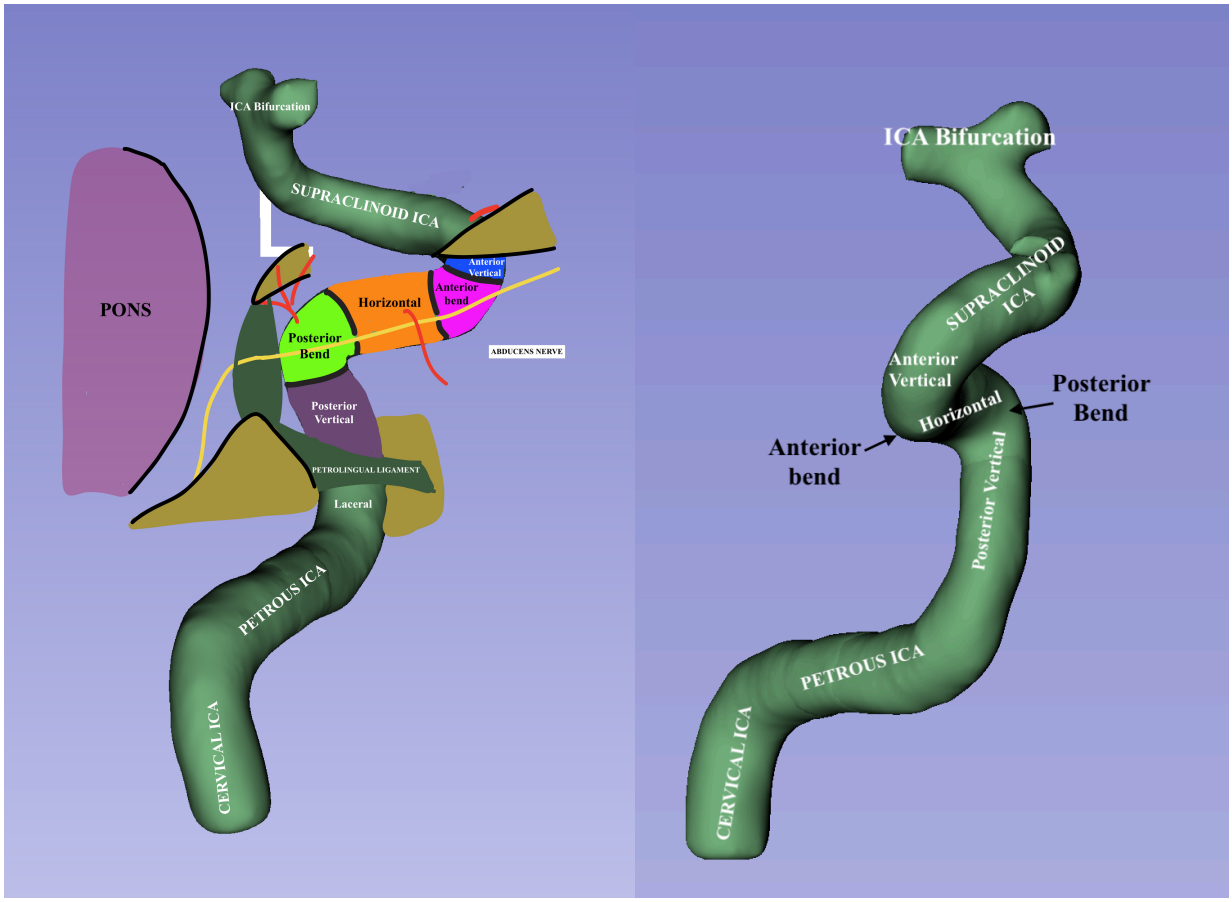
The ICA is divided into 7 segments as per the boutelier's classification (1996): (32) (33)

- C1 (Cervical): Entry of the ICA from it's origin at the bifurcation of CCA to it's entry into the carotid foramen at the base of skull
- C2 (Petrous): The part of the iCA within the carotid canal in the petrous part of the temporal bone. The origin of the caroticotympanic artery is a good landmark for the end of this segment.
- C3 (Laceral): The part of ICA from it's exit from the carotid canal to the posterior margin of foramen lacerum at the inferior margin of petrolingual ligament.
- C4 (Cavernous ICA): It begins at the superior margin of the petrolingual ligament to the proximal dural ring. This part of the ICA has two parts. An initial *ascending part* till the origin of the meningohypophyseal trunk where it turns horizontal. And a horizontal cavernous part from the exit of the meningohypophyseal trunk till the origin of the inferolateral trunk/ proximal dural ring.
- C5 (Clinoid): This is the part of the ICA between the proximal dural ring and origin of the ophthalmic artery.
- C6 (Ophthalmic): This segment is present between the ophthalmic artery and origin of PCOM artery.
- C7 (Communicating segment): This is the terminal segment of ICA starting at the origin of PCOM till it's bifurcation into MCA and ACA.

Inoue et al (34) classified intracavernous ICA into 5 segments morphologically

1. Posterior Vertical Segment
2. Posterior Bend
3. Horizontal segment

4. Anterior bend
5. Anterior vertical segment



MATERIALS AND METHODOLOGY

Design: Retrospective radio anatomical study.

Inclusion Criteria: Patients who have undergone MR TOF as part of pre operative work up for MMD are included in the study.

Exclusion Criteria: Incomplete imaging or advanced disease that precludes accurate measurements.

DATA COLLECTION PROCEDURES:

This is a retrospective radio-anatomical study. Data available in the hospital electronics medical records and PACS will be used for this study and will involve taking relevant measurements from MR TOF images of patients who were admitted at SCTIMST for moyamoya disease and a cohort of patients with non MMD pathologies undergoing MR TOF as controls like vasculitis, stroke, atherosclerotic disease, etc.

In our study, we compare the ICA morphometric data between the above two groups, analyse if there's a correlation between the degree of morphometric variation and severity of MMD Suzuki grading.

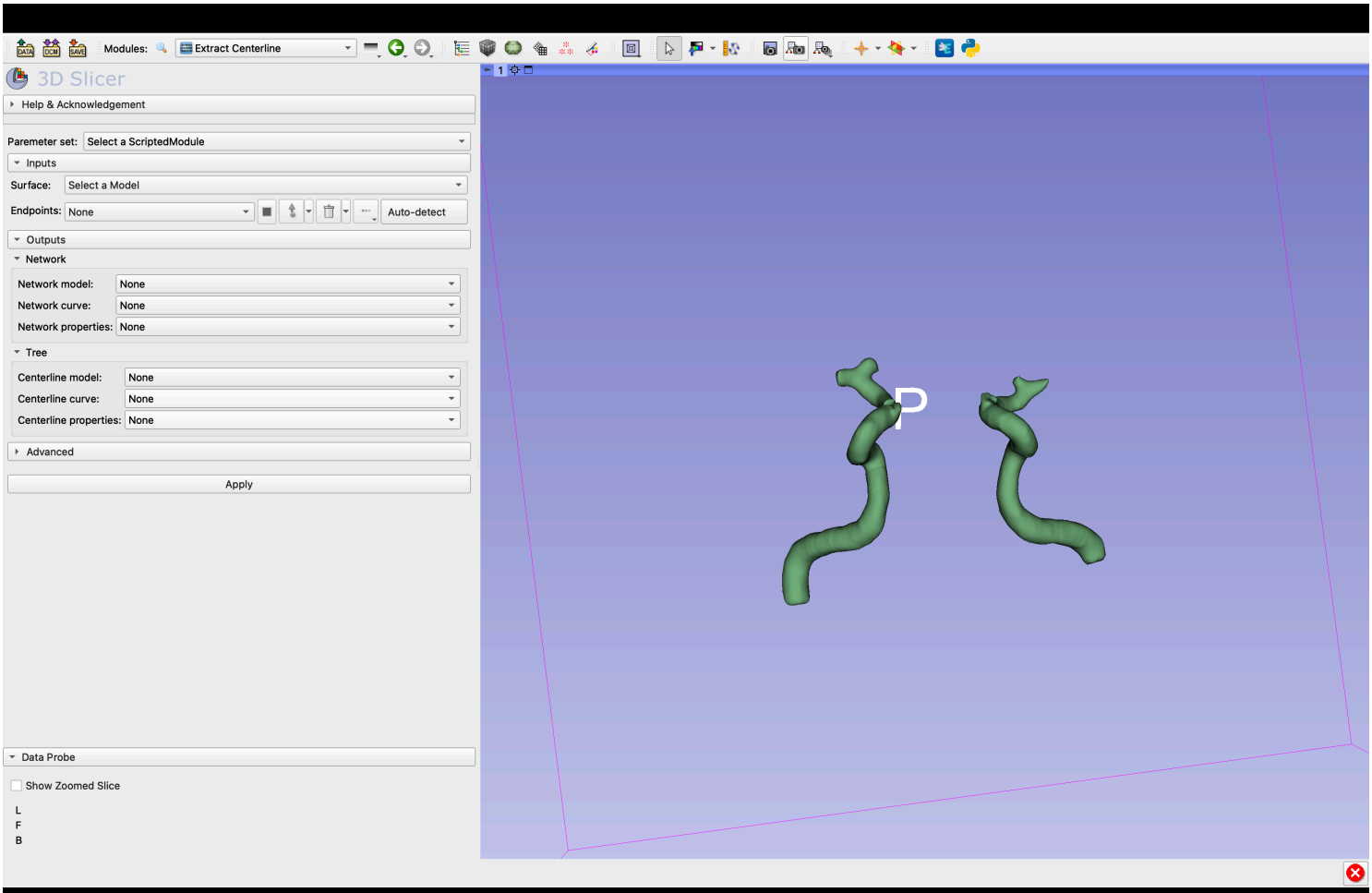
The different measurements we studied are:

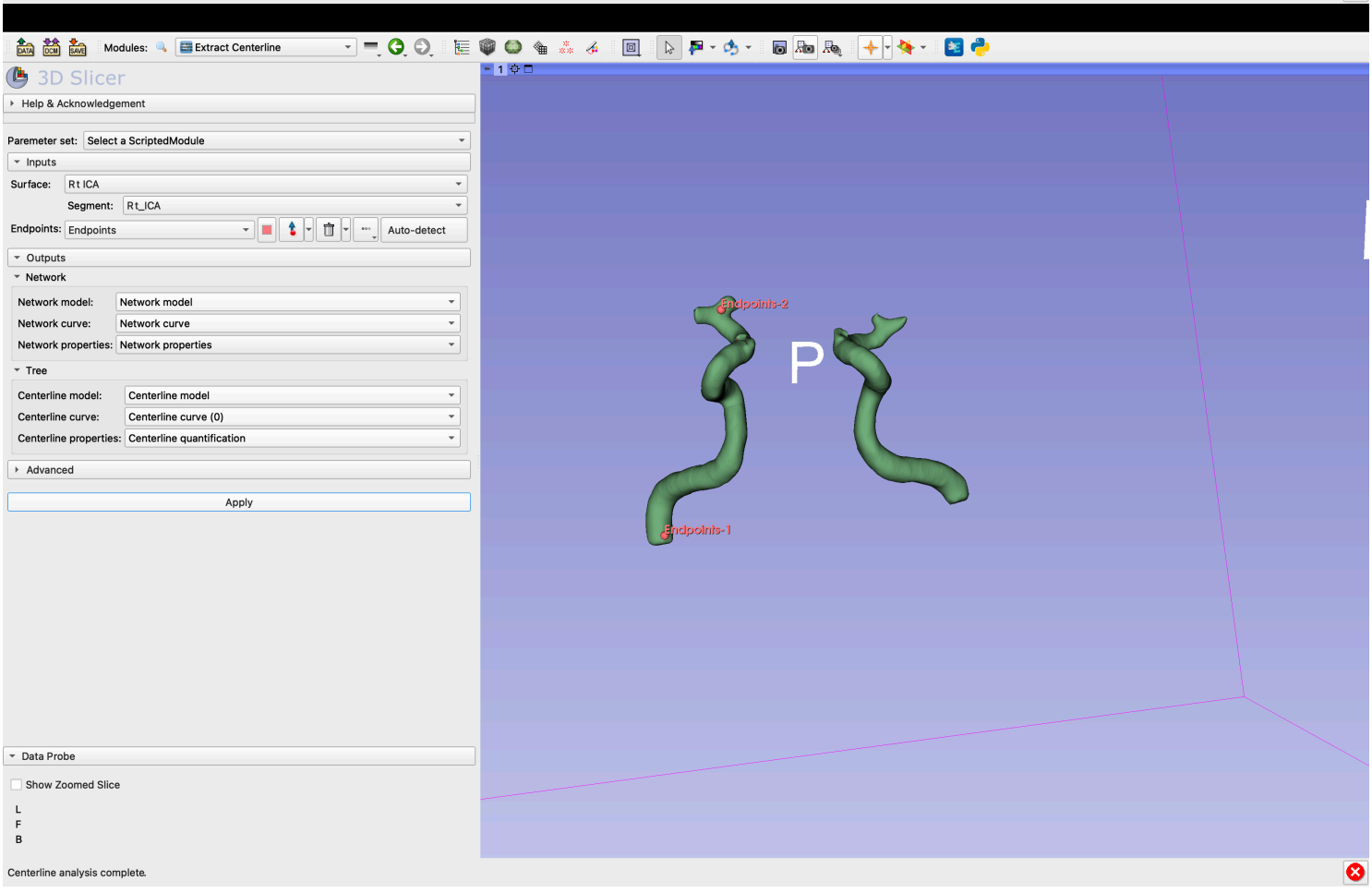
- **Angles:**
- Sagittal plane-
    - Cavernous ICA - Supraclinoid ICA angle,
    - Posterior Bend Angle (At the junction of the paraclival and cavernous segment)
- **Distance**
    - ICA to ICA distance i.e inter carotid distance at different levels
    - Petrous ICA (at level of head of mandible) to Clinoidal ICA (at level of ophthalmic artery) distance.

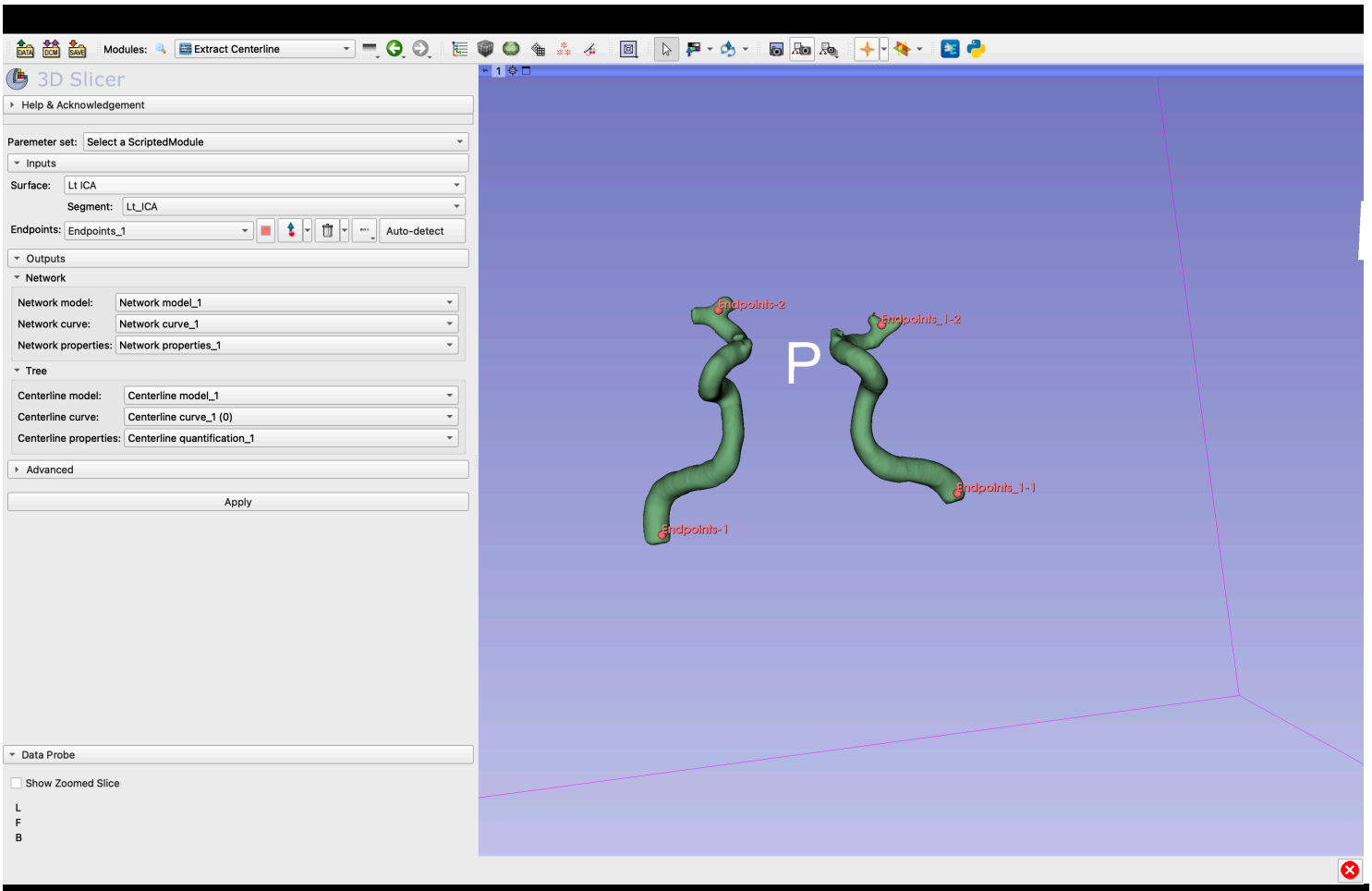
  - Actual Distance (AD)- This measured the length of ICA between these 2 points.
  - Linear Distance (LD)- This is the shortest distance between the above 2 points.
- **Tortuosity** of ICA (measured between the mid-level of head of mandible to level of origin of ophthalmic artery)
- [(Actual Distance/ Linear Distance)-1]*100
- **Base Vertex height of ICA curves:**
  - A straight line is drawn from origin of Petrous ICA (at level of head of mandible) to clinoid ICA at level of origin of ophthalmic artery i.e ***LD line***
  - In the saggital plane there are clearly 4 curves the intracranial ICA makes between the above 2 points, in relation to the above line.
  - The perpendicular distance between the above line and the apex of the said curves is measured, ***Base Vertex height (BVH)***. If the apex is anterior to the LD line, the value is assigned a positive sign and if the apex of the curve is posterior to the LD line, a negative sign is assigned to the measured value.
  - These short perpendicular lines give us a measure of the tortuosity at each segment.
  - A total of 4 BVH lines were measured. BVH 1 and BVH 3 for curves with convexity posteriorly and BVH 2 and BVH 4 for curves with convexity anteriorly.

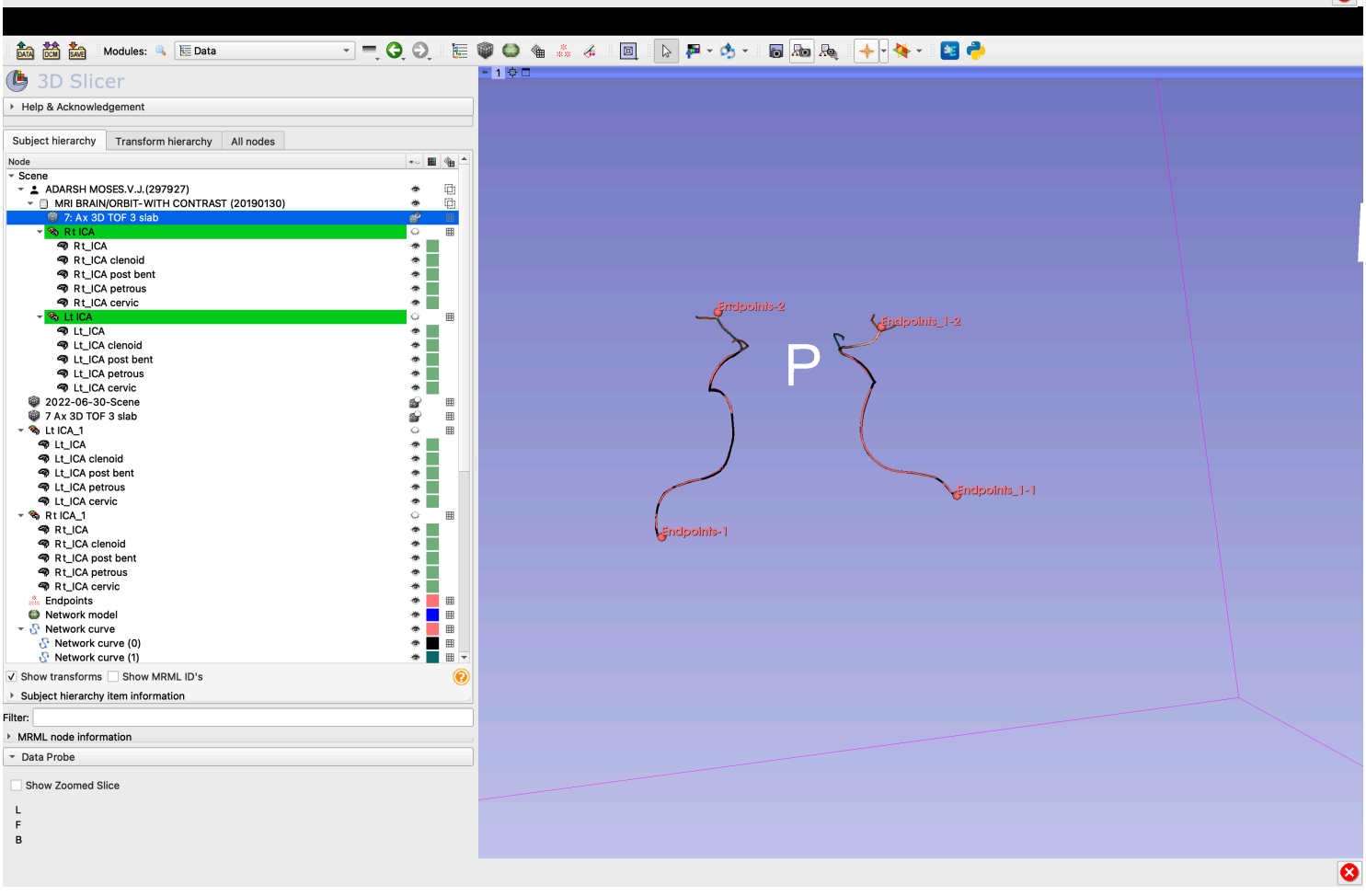
A list of cases and controls were made from the hospital EMR. The dicom files were extracted into cds. Following this, both the technical engineer incharge of segmenting and the PIs incharge of measurements were blinded to the aforementioned list and were not aware of the diagnosis of the patients to whom the images belonged to.

3D Slicer©


Modules:
Extract Centerline
3D Slicer
Help & Acknowledgement
Paremeter set:
Select a ScriptedModule
Inputs
Surface:
Select a Model
Endpoints:
None
Auto-detect
Outputs
Network
Network model:
None
Network curve:
None
Network properties:
None
Tree
Centerline model:
None
Centerline curve:
None
Centerline properties:
None
Advanced
Apply
Data Probe
Show Zoomed Slice
L
F
B
P


Modules:
Extract Centerline
3D Slicer
Help & Acknowledgement
Paremeter set:
Select a ScriptedModule
Inputs
Surface:
Rt ICA
Segment:
Rt_ICA
Endpoints:
Endpoints
Auto-detect
Outputs
Network
Network model:
Network model
Network curve:
Network curve
Network properties:
Network properties
Tree
Centerline model:
Centerline model
Centerline curve:
Centerline curve (0)
Centerline properties:
Centerline quantification
Advanced
Apply
Data Probe
Show Zoomed Slice
L
F
B
Endpoints-2
P
Endpoints-1
Centerline analysis complete.


Modules:
Extract Centerline
3D Slicer
Help & Acknowledgement
Paremeter set:
Select a ScriptedModule
Inputs
Surface:
Lt ICA
Segment:
Lt_ICA
Endpoints:
Endpoints_1
Auto-detect
Outputs
Network
Network model:
Network model_1
Network curve:
Network curve_1
Network properties:
Network properties_1
Tree
Centerline model:
Centerline model_1
Centerline curve:
Centerline curve_1 (0)
Centerline properties:
Centerline quantification_1
Advanced
Apply
Data Probe
Show Zoomed Slice
L
F
B
P
Endpoints-2
Endpoints_1-2
Endpoints_1-1
Endpoints-1


Modules:
Data
3D Slicer
Help & Acknowledgement
Subject hierarchy
Transform hierarchy
All nodes
Node
Scene
ADARSH MOSES.V.J.(297927)
MRI BRAIN/ORBIT- WITH CONTRAST (20190130)
7: Ax 3D TOF 3 slab
Rt ICA
Rt_ICA
Rt_ICA clenoid
Rt_ICA post bent
Rt_ICA petrous
Rt_ICA cervic
Lt ICA
Lt_ICA
Lt_ICA clenoid
Lt_ICA post bent
Lt_ICA petrous
Lt_ICA cervic
2022-06-30-Scene
7 Ax 3D TOF 3 slab
Lt ICA_1
Lt_ICA
Lt_ICA clenoid
Lt_ICA post bent
Lt_ICA petrous
Lt_ICA cervic
Rt ICA_1
Rt_ICA
Rt_ICA clenoid
Rt_ICA post bent
Rt_ICA petrous
Rt_ICA cervic
Endpoints
Network model
Network curve
Network curve (0)
Network curve (1)
Show transforms
Show MRML ID's
Subject hierarchy item information
Filter:
MRML node information
Data Probe
Show Zoomed Slice
L
F
B
P
Endpoints-2
Endpoints_1-2
Endpoints_1-1
Endpoints-1

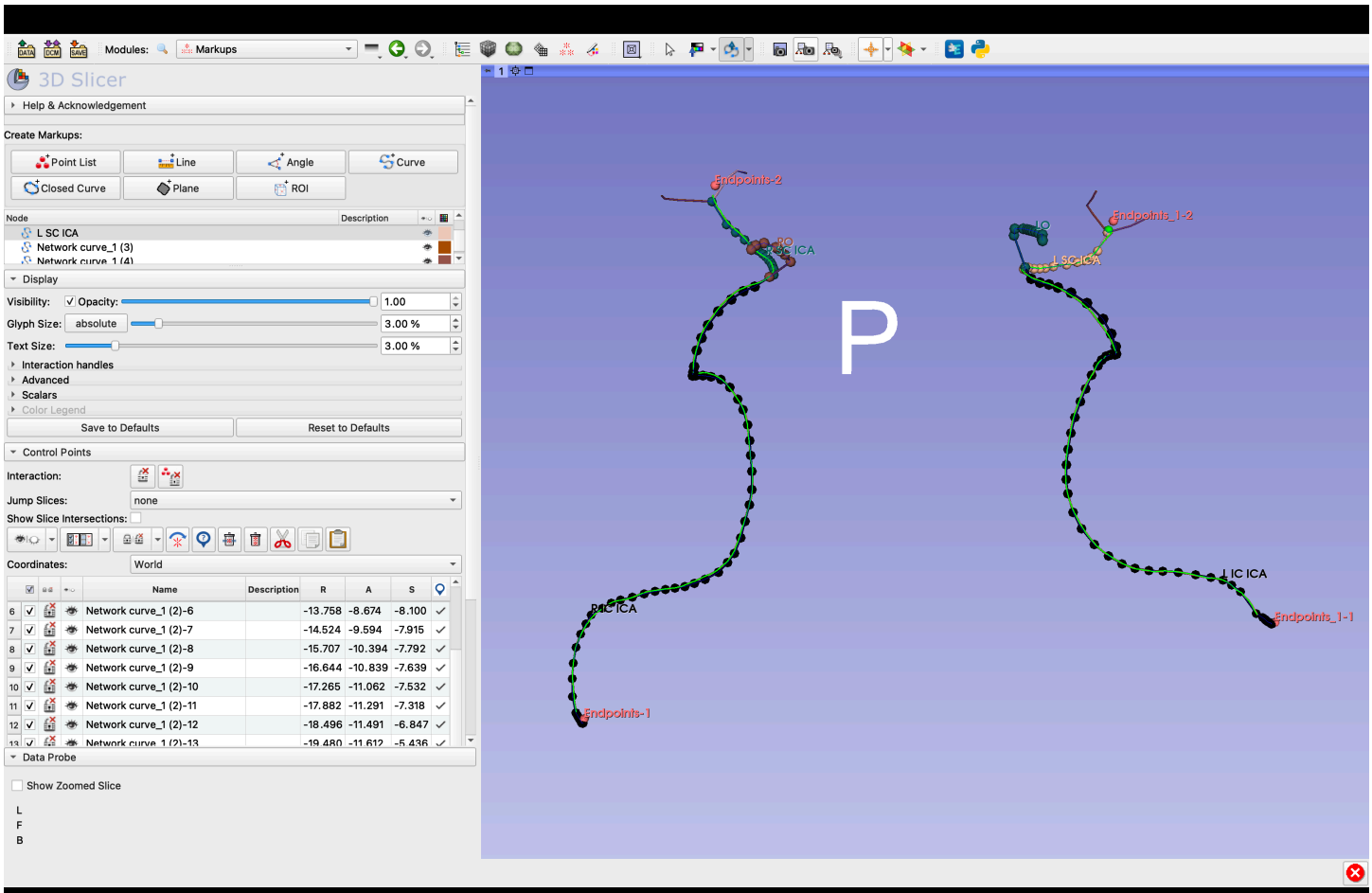
In order to get an accurate estimation of the course of the intracranial ICA in 3D space, we used an open source software known as **"3D Slicer©"** ((35)). 3D Slicer © is a robust application for the visualization and analysis of biomedical image data. The source file in dicom format was uploaded into the 3D slicer © software and reconstructed to produce a 3D image of ICA in space. The soft tissue other than ICA was subtracted to isolate only the 3D image of ICA.

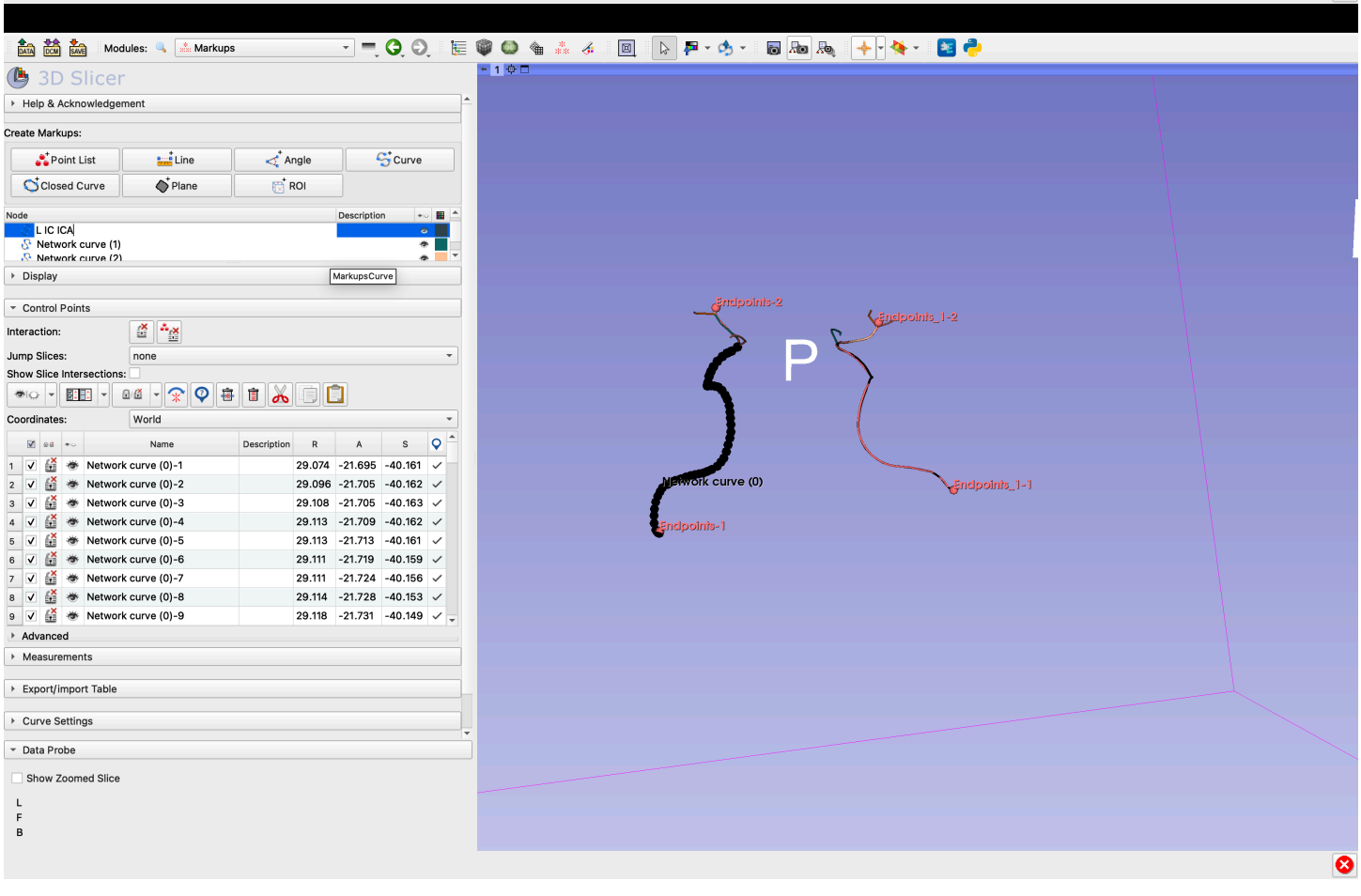
Here, image segmentation is the process of dividing a digital image into different subdivisions or image segments or image regions . Image segmentation is required for the simplification of the data set in hand and for its meaningful analysis. Image segmentation can be done using various techniques and algorithms depending on the requirement. In the present study, *manual thresholding* is done as it is handier in situations demanding more manual interventions. Manual thresholding is done by setting the maximum and minimum HU values of the area of interest which is the ICAs.

The 3D reconstruction is generated once the ICAs are segmented. The VMTK (Vascular modelling toolkit) extension in the 3D© slicer is exploited to develop the centreline of the ICAs. The quantifications like length, tortuosity and radius of curvature are calculated based on the developed centrelines.

The ICA image thus segmented and trimmed is used for central line extraction. This process extracts the geometric central line of the vessel in 3D Space. Presence of Glyphs (enlarged points along the central line) adjustable to a desirable size was paramount in achieving higher accuracy in measurements.

It needs to be understood that measurements were made on a saggital or axial or coronal image series where the central line was superimposed on the ICA. This is important to understand that in 3D space true lateral or horizontal or vertical measurements are difficult to achieve due to the ascent of the ICA along different planes. Hence, glyph to glyph measurements on the 3D space is not likely to yield angles and measurements that is true to the plane it is being measured in.

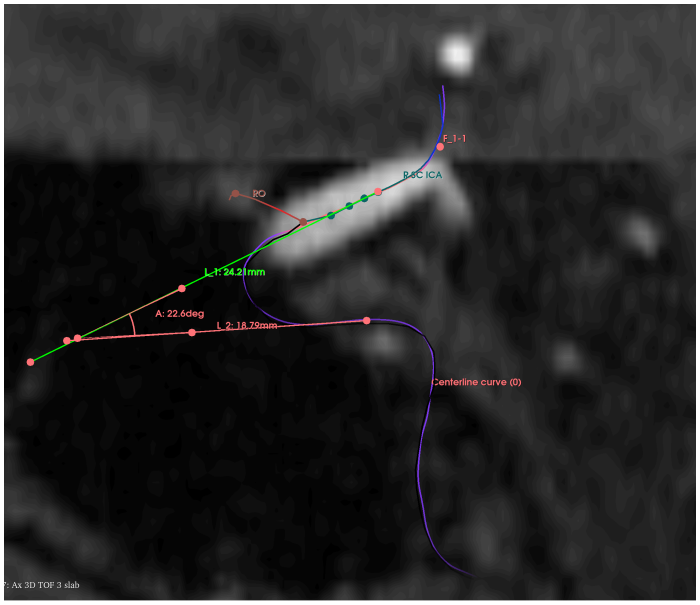

Modules: Markups
3D Slicer
Help & Acknowledgement
Create Markups:
Point List
Line
Angle
Curve
Closed Curve
Plane
ROI
Node
Description
L SC ICA
Network curve_1 (3)
Display
Visibility:
Opacity:
1.00
Glyph Size:
absolute
3.00 %
Text Size:
3.00 %
Interaction handles
Advanced
Scalars
Color Legend
Save to Defaults
Reset to Defaults
Control Points
Interaction:
Jump Slices:
none
Show Slice Intersections:
Coordinates:
World
Name
Description
R
A
S
6 Network curve_1 (2)-6 -13.758 -8.674 -8.100
7 Network curve_1 (2)-7 -14.524 -9.594 -7.915
8 Network curve_1 (2)-8 -15.707 -10.394 -7.792
9 Network curve_1 (2)-9 -16.644 -10.839 -7.639
10 Network curve_1 (2)-10 -17.265 -11.062 -7.532
11 Network curve_1 (2)-11 -17.882 -11.291 -7.318
12 Network curve_1 (2)-12 -18.496 -11.491 -6.847
Data Probe
Show Zoomed Slice
L
F
B
Endpoints-2
Endpoints_1-2
L IC ICA
Endpoints_1-1
Endpoints-1
P


Modules: Markups
3D Slicer
Help & Acknowledgement
Create Markups:
Point List
Line
Angle
Curve
Closed Curve
Plane
ROI
Node
Description
L IC ICA
Network curve (1)
Display
MarkupsCurve
Control Points
Interaction:
Jump Slices:
none
Show Slice Intersections:
Coordinates:
World
Name
Description
R
A
S
1 Network curve (0)-1 29.074 -21.695 -40.161
2 Network curve (0)-2 29.096 -21.705 -40.162
3 Network curve (0)-3 29.108 -21.705 -40.163
4 Network curve (0)-4 29.113 -21.709 -40.162
5 Network curve (0)-5 29.113 -21.713 -40.161
6 Network curve (0)-6 29.111 -21.719 -40.159
7 Network curve (0)-7 29.111 -21.724 -40.156
8 Network curve (0)-8 29.114 -21.728 -40.153
9 Network curve (0)-9 29.118 -21.731 -40.149
Advanced
Measurements
Export/import Table
Curve Settings
Data Probe
Show Zoomed Slice
L
F
B
Endpoints-2
Endpoints_1-2
Network curve (0)
Endpoints_1-1
Endpoints-1
P

We perform the same with the projection of the central line along different planes to measure angles. Thus, we are able to achieve a true sagittal plane measure of angles at cavernous supraclinoid segments and at the paraclival-cavernous segments.

A) Angles: Angles were measured following traditional rules. While measuring the 2 angles mentioned, the line passing through glyphs of the cavernous ICA was fixed and angle was measured in an anti clock wise direction to the other line. When carotid siphon was closed, there was an apparent divergence resulting in negative supraclinoid cavernous ICA angles measured behind the clinoid segment in the saggital plane.

A) Cavernous- supraclinoid ICA angle-

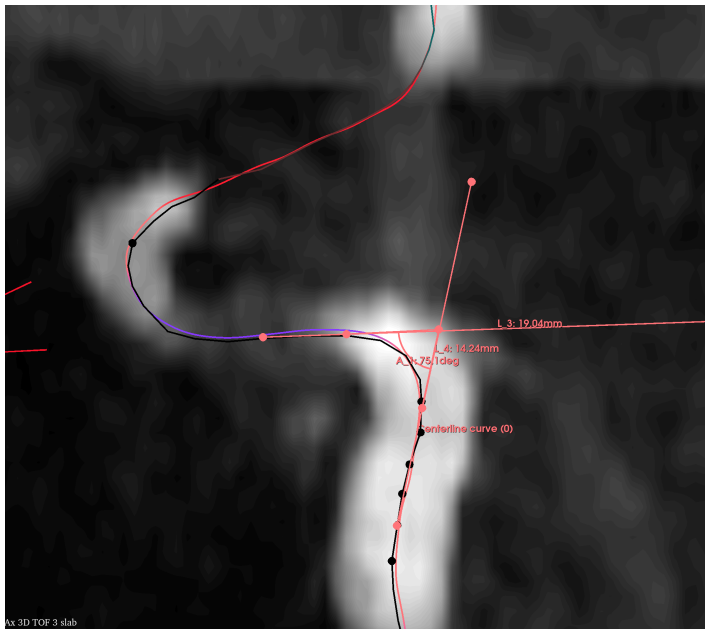


- A line passes through as many glyphs as possible along the course of the cavernous ICA

- A line passes through as many glyphs as possible along the course of the supraclinoid ICA (i.e distal to origin of ophthalmic artery
- Angle of intersection between the 2 lines measured.
- Consequently if the carotid siphon was open and the the two lines converged

anterior to the clinoid segment it was an acute angle, if the 2 lines were parallel the angle was 0 degrees and if the siphon was closed and the lines converged posterior to the clinoid segment the angle between the lines was a negative value.

B) Posterior bend angle



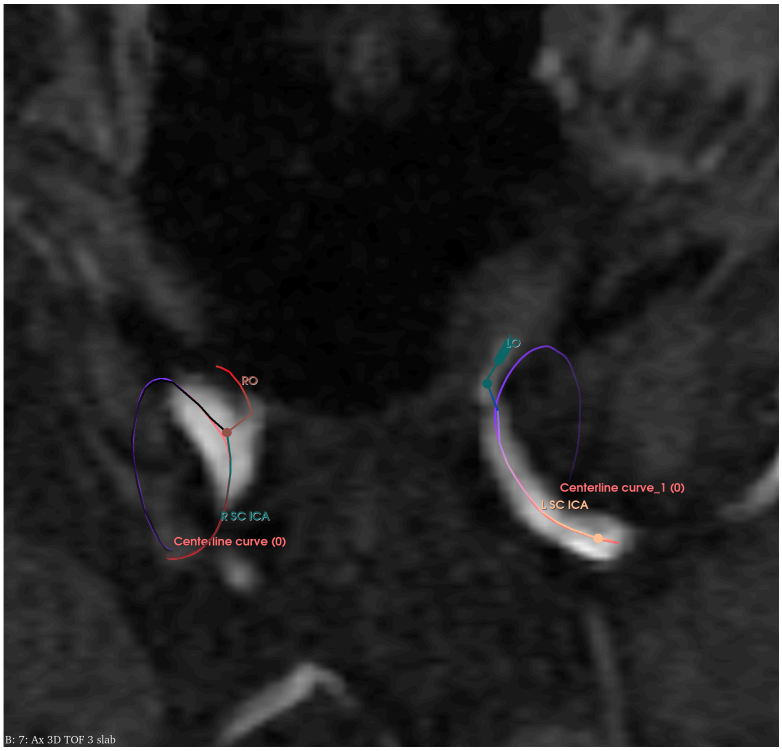
- A line passes through as many glyphs as possible along the course of the horizontal cavernous ICA
- A line passes through as many glyphs as possible along the course of the Paraclival ICA
- Angle of intersection between the 2 lines measured.
- Consequently if the the two lines converged posterior to the junction of paraclival and horizontal cavernous ICA transition it was an acute angle, and if the lines met anterior to the bend it was a negative angle.

B) Intercarotid distance (ICD)-

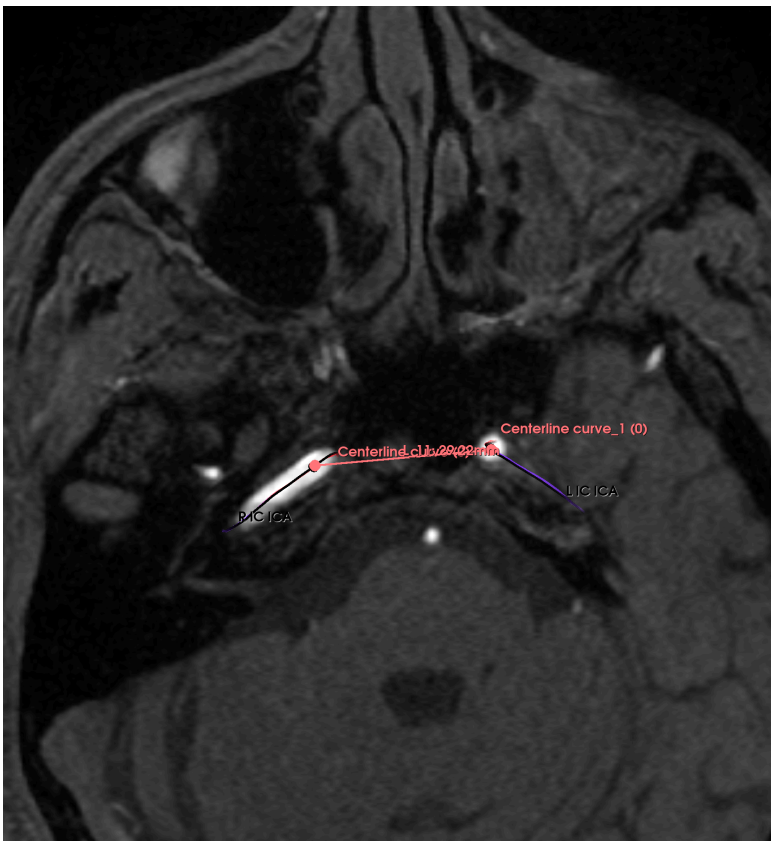
The distance between the ICA on either side was measured at 4 levels,

corresponding to specific landmarks on the TOF image.

1. ICD 1- Measured in the axial section at the level of the origin of ophthalmic

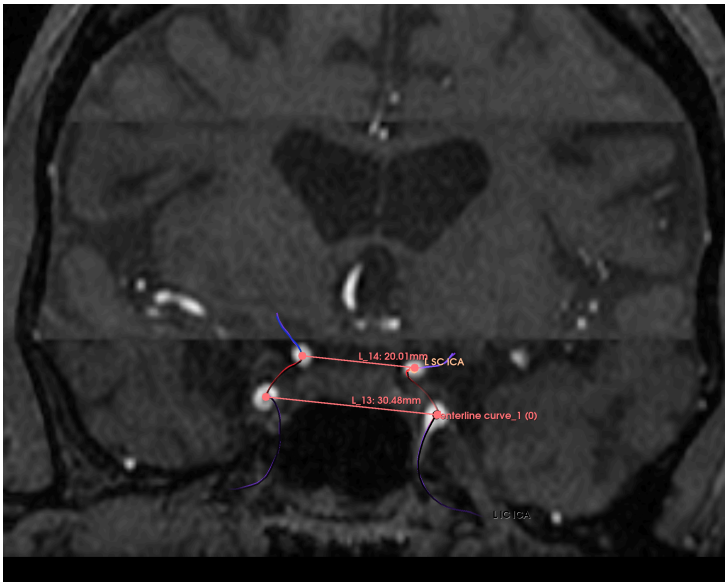


artery. In scans where origin of ophthalmic artery was not discernible on one side, the corresponding point to the level of origin on the opposite side was used to measure ICD 1. If ophthalmic artery was not discernible bilaterally, then ICD1 was not measured for the patient.



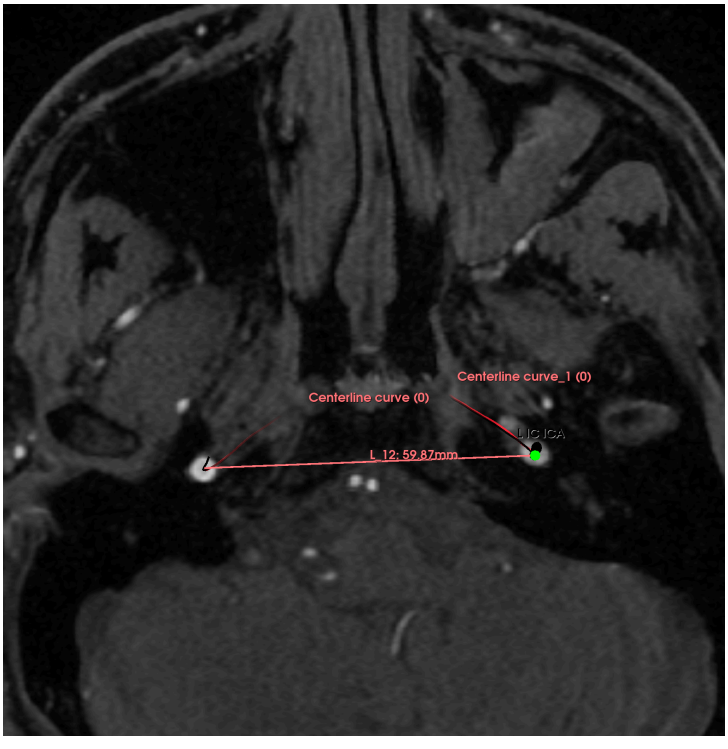
2. ICD 2- Measured in the axial section as the narrowest distance between the central lines of ICA on either side at the level of the internal acoustic meatus (IAM). The narrowest distance was necessary as in some cases the ICA turns lateral proximally in it's petrous course and we may have multiple glyph points to measure in a single axial section.

3. ICD 3- Measured in the coronal section at the level of the pituitary gland in the



sella, in a section visualising the pituitary stalk. The distance between the glyphs of cavernous ICA central lines was assigned as 3a and between those of the supraclinoid ICA was assigned as 3b. In cases where supraclinoid segment was not visualised, ICD 3b was left blank.

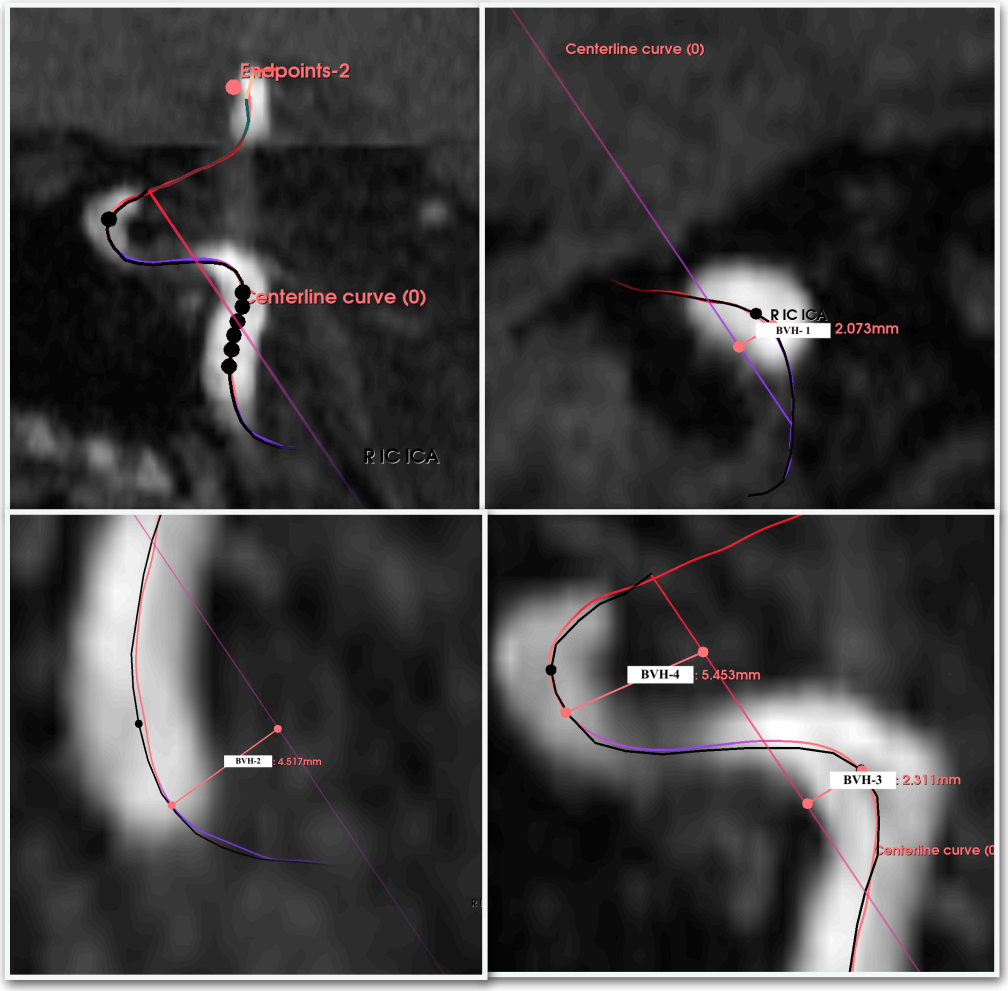
4. ICD 4- Measured in the axial section at the mid level of mandibular head. This



would reveal the distance between the 2 ICA's at this landmark

C) Linear distance(LD) and actual distance(AD) from petrous ICA (at mid level of mandibular head) to clinoidal ICA (at level of origin of ophthalmic artery). This will give us an idea of redundancy and tortuosity of the vessel.

D Base vertex Height (BVH) Lines:



- A straight line is drawn from origin of Petrous ICA (at level of head of mandible) to clinoid ICA at level of origin of ophthalmic artery i.e LD line.
- In the saggital plane there are clearly 4 curves the intracranial ICA makes between the above 2 points, in relation to the above line. 2 curves have their convexity directed anteriorly and 2 posteriorly.
- The perpendicular distance between the above line and the apex of the said curves is measured. If the apex is anterior to the line, the value is assigned a

positive sign and if the apex of the curve is posterior to the line, a negative sign is assigned to the measured value.

- These short perpendicular lines give us a measure of the individual curve at each segment.

The measurements were made by the principal investigator and technical assistant and vetted by the co- principal investigator to reduce errors.

DATA ANALYSIS:

Data analysis was made by the Principal and Co-Principal investigators with the help of a statistical software (SPSS). A statistician was consulted to arrive at relevant values. The threshold for statistical significance was set at $p < 0.05$. The clinical significance and relevance was discussed between the PI, Co-PI and co-investigators as part of the study discussion. Gender was not recorded. No observation was made/recorded for class, caste, ethnicity and race.

While measuring angles (both supraclinoid-cavernous angle and posterior bend angle) if the carotid siphon was open and the the two lines converged anterior to the clinoid segment it was a positive angle, and if the siphon was closed and the lines converged posterior to the clinoid segment the angle between the lines was a negative angle. Similarly, while measuring PBA if the the two lines converged posterior to the junction of paraclival and horizontal cavernous ICA transition it was an acute angle, and if the lines met anterior to the bend it was a negative angle.

The lowest negative angle within the entire cohort (i.e both cases and control) was assigned as $x = 0$ and the values for each patient was assigned reassigned ($y + x$). This way we were able to run the Mann Whitney U test as the data distribution between cases and control was not normal and arrived at the p value.

RESULTS

We assessed a total of 114 patients and a total of 207 ICAs. The patients of Moyamoya disease were categorised into adults and children.The comparisons were between the adult group of MMD and controls as the age difference and size of skull was a confounding factor if the children MMD group was used. This also included normal side ICA of 3 patients with unilateral moyamoya disease and 1 patient with secondary MMD on the left side.
The control group included TOF MR images of patients with diseases other than moyamoya disease like vasculitis, stroke, aneurysms and AVMs and normal TOF MR image of patients with normal angiogram.

Type	Total No of patients	Total No of ICA	Mean Age
Adults with MMD	**30**	**50**	**32.83**
Children with MMD	21	40	7.77
Controls	67	125	44.47
Total	118	215	

ANGLES

1. Cavernous ICA- Supraclinoid ICA angle:

Closed siphons resulted in negative angles. So we removed the negative values in order to estimate the mean and median between the remaining values.
To calculate p value, the lowest from that group (i.e adult MMD/control/ children MMD) was made 0 and the difference was added to all the values of that group. The p value was then calculated using Mann Whitney U test.

These were found to be significant when the children MMD group and control group were compared to the adult MMD group.
The mean angle in children with MMD was 50 degrees as opposed to 39.20 degrees is adult patients with MMD. The mean angle in controls was 30.05 degrees.

Cavernous ICA-Supraclinoid ICA angle in	Mean	Median	Max	Min	P value	U value	Z Score
Adult MMD	39.20	38.3	100.4	-25			
Children MMD	57.03	68.5	102	-27	0.006	416.5	-2.752
Controls	30.05	29.15	117.5	-54.3	0.001	2037	-3.266

2. Posterior bend angle:

We removed the negative values in order to estimate the mean and median between the remaining values.

To calculate p value, the lowest from that group (i.e adult MMD/control/ children MMD) was made 0 and the difference was added to all the values of that group. The p value was then calculated using Mann Whitney U test.

There was a significant difference in the posterior bend angle between the ICA of adult moyamoya disease and the control group. Posterior bend angle was not significantly different between the adult and children MMD cases. The mean PBA was 110.08 in adults and 85.23 in controls.

Posterior bend ICA angle in degrees

Adult MMD vs other categories	Mean	Median	Max	Min	P value	U Value	Z Score
Adult MMD	110.08	114.35	167.2	-22.8			
Children MMD	122.46	126.9	177	56.4	0.149	908.5	-1.443
Controls	85.23	89.8	161.3	-16.9	<0.01	2072.5	-4.239

DISTANCE

3. Intercarotid distance

    1. ICD 1- measured at the level of the origin of opthalmic artery was significantly different between adult MMD and Children. Similarly, between controls and adult MMD the difference was significant. The mean values were 21.22, 19.33 and 19.72 for adult MMD, children MMD and controls respectively.

ICD 1

Adult MMD vs other categories	Mean	Median	Max	Min	P value	U Value	Z Score
Adult MMD	21.22	21.22	25.78	15.89			
Children MMD	19.335	19.51	25	14.32	0.01828	152.5	-2.593
Controls	19.72	19.05	30.76	14.61	0.010	553	-2.593

    2. ICD2- When inter carotid distance was measured at the level of the IAC, there was no significant difference between adult MMD and controls, nor between adult MMD and children MMD groups.

ICD 2

Adult MMD vs other categories	Mean	Median	Max	Min	P value	U value	Z score
Adult MMD	26.403	25.65	32.23	21.08			
Children MMD	25.50	25.41	31.35	21.61	0.690	229	-0.398
Controls	25.75	25.41	41.51	15.27	0.396	720.5	-0.848

3. ICD 3A- Intercarotid distance between the cavernous ICA at the level of the pituitary gland was not significant between the adult MMD cases and the controls nor between adult MMD cases and children MMD cases.

ICD 3a

Adult MMD vs other categories	Mean	Median	Max	Min	P value	U value	Z score
Adult MMD	23.59	22.77	51.15	15.14			
Children MMD	22.29	22.61	25.13	18.62	0.564	180.5	-0.579
Controls	21.66	21.73	30.32	13.03	0.169	626	-1.374

4. ICD 3B- Intercarotid distance between the supraclinoid CA at the level of the pituitary gland was found to be significantly different between the adult MMD cases and the controls, as well as between adult MMD cases and children MMD cases.

ICD 3b

Adult MMD vs other	Mean	Median	Max	Min	P value	U value	Z Score
Adult MMD	19.85	20.07	23.61	15.01			
Children MMD	19.24	19.43	24.18	14.59	0.00804	44	2.65
Controls	18.68	18.27	25.19	14.35	0.02	419	-2.182

5. ICD 4- Intercarotid distance between the petrous ICA at the level of the midlevel of mandibular head was significant between the adult MMD cases and control as well as between adult and children MMD groups.

ICD 4

Adult MMD vs other categories	Mean	Median	Max	Min	P value	U Value	Z Score
Adult MMD	56.25	57.01	73.85	46.21			
Children MMD	49.14	48.61	56.52	41.81	<0.01	76	-3.516
Controls	56.98	57.92	66.79	30.84	0.02	419	-2.182

4. Tortuosity

The difference in tortuosity of ICA was significant against both children group of MMD and control group. The mean toruosity of the adult MMD group was 0.2479 while that of the children group was 0.13 and of the control group was 0.41.

Tortuosity

Adult MMD vs other	Mean	Median	Max	Min	P value	U Value	Z Score
Adult MMD	0.2479	0.208	0.6776	0.0432			
Children MMD	0.13	0.1291	0..3264	0.0306	<0.01	590	-3.652
Controls	0.41	0.34	5.024	0.1256	<0.01	1625.5	5.49535

5. Base Vertex Height:

1. BVH 1: the difference in BVH-1 value was significant between the adult and children moyamoya group. However, the difference was not statistically significant between the adult MMD group and controls

BVH-1

Adult MMD vs other categories	Mean	Median	Max	Min	P value	U Value	Z Score
Adult MMD	-1.79	-1.989	0.6544	-4.122			
Children MMD	-1.27	-1.058	0	-4.622	0.006	533	-2.754
Controls	-2.27	-1,917	4.885	-11.65	0.743	3004	-0.329

2. BVH 2: the difference in BVH-2 value was significant between the adult MMD group and control group. However, the difference was not statistically significant between the adult MMD group and children MMD group.

BVH-2

Adult MMD vs other	Mean	Median	Max	Min	P value	U Value	Z Score
Adult MMD	2.033	2.038	5.044	-1.051			
Children MMD	1.699	1.8245	3.980	-0.86	0.352	761	-0.931
Controls	2.717	3.002	6.494	-7.209	0.02	3194	2.312

3. BVH 3: the difference in BVH 3 value was significant between the adult MMD group and control group as well as adult MMD group and children MMD group.

BVH-3

Adult MMD vs other categories	Mean	Median	Max	Min	P value	U Value	Z Score
Adult MMD	−2.67	-2.720	1.389	-8.955			
Children MMD	-1.29	-1.724	5.746	-5.551	0.039	602	-2.068
Controls	-3.28	-3.813	3.559	-9.580	0.05	2304	-1.906

4. BVH 4: The difference in BVH 4 value was significant between the adult MMD group and control group. However, the difference was not statistically significant between the adult MMD group and children MMD group.

BVH-4

Adult MMD vs other categories	Mean	Median	Max	Min	P value	U Value	Z score
Adult MMD	1.6022	1.676	4.628	-0.8			

BVH-4

Adult MMD vs other categories	Mean	Median	Max	Min	P value	U Value	Z score
Children MMD	1.202	2.121	3.670	-0.6571	0.105	557	-1.623
Controls	2.87	2.81	6.455	0	<0.01	1463	-4.680

6. Linear distance measured between the 2 fixed points for tortuosity measurements, i.e from mid level of head of mandible to origin of ophthalmic artery was measured in the above 3 groups. The difference in value for measured linear distance was significant between the adult MMD group and control group as well as adult MMD group and children MMD group.

LD

Adult MMD vs other	Mean	Median	Max	Min	P value	U Value	Z Score
Adult MMD	38.87	38.94	47.30	31.86			
Children MMD	35.47	35.7	42.57	28.3	<0.01	388.5	-4.024
Controls	41.0325	41.17	50.37	30.44	<0/01	1501	-3.813

7. Actual distance measured between the 2 fixed points for tortuosity measurements, i.e from mid level of head of mandible to origin of ophthalmic artery was measured in the above 3 groups. The difference in value for measured actual distance was significant between the adult MMD group and control group as well as adult MMD group and children MMD group.

AD

Adult MMD vs other	Mean	Median	Max	Min	P value	U Value	Z Score
Adult MMD	47.1	46.52	64.43	33.89			
Children MMD	39.33	39.755	49.83	18.72	<0.01	357	-5.601
Controls	52.76	52.62	68.27	24.31	<0.01	1636	-5.399

DISCUSSION

The motivation for the work put into this dissertation are two of the earlier papers published by the co-principal investigator. The first of which was a discussion on the effect of hemodynamic stress due to a higher cavernous-supraclinoid angle and reduced tortuosity in moyamoya disease on vascular remodelling that occurs in the same(7). In the study methodology, the angles were measured between the lines drawn through mid point of diameters of cavernous and supraclinoid segment on DSA in saggital plane. We intended to obtain the true central line for a more accurate representation using 3D slicer© technology. The mean cavernous- supraclinoid ICA angle in the above mentioned study was 69.7 degrees in MMD and 40.5 degrees in control group, the difference being statistically significant. However, in our study the mean cavernous- supraclinoid ICA angle was 39.20 degrees in adult MMD, 57.03 degrees in children with MMD and 30.05 degrees in controls. The difference was significant in both the studies. In the same paper, CAD model of a normal ICA was subjected to increasing cavernous supraclinoid angle and CFD analysis was carried out to arrive at the wall shear stress (WSS) at ICA bifurcation. The wall shear stress was found to be directly proportional to the cavernous supraclinoid ICA angle amongst the 4 variations measured. Kim T et al (8) in their study created two 3D models, one for MMD patients and one for control and ran CFD analysis to find a higher flow velocity and WSS at terminal ICA bifurcation and proximal ICA and MCA. Postmortem histopathological examination of intracranial ICA belonging to deceased patients with MMD revealed fibrocellular intimal thickening at diseased areas, proliferative smooth muscle cells with no atherosclerosis / inflammation seen(24) (36). The supraclinoid ICA in MMD was postulated to have an increased mobility in the subarachnoid cisternal space ‘like an air dancer’ due to decreased vessel wall strength resulting in the fibrocellular intimal thickening going haywire(7). The increased wall shear stress combined with an abnormal vessel mobility results in a compounded effect that leads to concentric luminal narrowing. The authors suggested that the erosion of these endothelial cushions due to the increased WSS

might lead to repeated embolism resulting in recurrent TIA/strokes seen in these patients.

A second publication by the co-PI, a systematic review by B.J. Sudhir et al (2021) proposed a mechanobiological hypothesis on the pathogenesis of moyamoya disease (MMD) (6). In this review, six key factors i.e arterial tortuosity, vascular angles, wall shear stress, molecular factors, blood rheology and blood vessel wall strength were implicated in the loss of balance in vascular homeostasis in MMD. To further the evidence gathered, in the review a retrospective radio anatomical study was devised in order to measure ICA morphometrics like angles, various distances and tortuosity as mentioned in the methodology of this study. Vascular modelling during embryogenesis and remodelling during life is described to be part of a continuum. Syndromic moyamoya disease is characterised by craniofacial deformities as a common presentation. This may implicate altered growth kinetics of the skull, skull base and the resultant effect of these growth kinetic vectors on ICA development. On the contrary, one could surmise that the altered growth kinetics of ICA which is the main blood supply in the growing embryo, can result in abnormal craniofacial development in MMD due to a tethering effect by the foreshortened ICA. Kim T et al (8) found shorter actual distance of the vessel measured from carotid canal to the carotid siphon in addition to higher cavernous supraclinoid ICA angles. In corroboration with their findings, we found a significant difference between not only the actual length of the ICA from the mid level of the mandibular head to the ophthalmic artery, but also reduced linear distance between the same two points in 3D space. This means that there is a reduced toruosity indeed, but the magnitude of the reduced toruosity is understated despite it’s statistical significance, due to the reduced linear distance between the two points mentioned above. This could imply one of two things as mentioned above, that altered growth kinetics overall result in reduced tortuosity, or that the reduced tortuosity is in itself a tethering factor causing subtle retardation in craniofacial development. The RNF213 gene variant R4810.K is

definitively implicated in patients with MMD and is associated with loss of ICA tortuosity(22). This was studied in Zebra fish embryos. There was a delay in the loss of acuteness of the head-trunk angle in zebra fish embryos with antisense mediated knockdown of RNF213(37). It was postulated that there must be dyssynchrony in the development of cranial vasculature with delay in the straightening of craniocervical flexure resulting in loss of ICA tortuosity, altered cavernous- supraclinoid angle, posterior bend angle etc. (6) Thus, loss of synchrony and altered growth kinetics between ICA development and maturation with craniofacial/skullbase development may explain the significant difference seen in posterior bend angle, linear distance, inter carotid distance etc in our study.

Inter-carotid distance (ICD) has not been measured in patients with MMD. Sawant N et al (11) measured ICD in pediatric patients with no skull base pathology. ICD was measured between medial walls of ICA and the narrowest ICD was seen at the level of the proximal dural ring measuring (14.6±2.4mm). ICD in children was also measured at cavernous ICA (16.73±2.7 mm) and paraclival ICA (short vertical, at the cephalic turn of petrous ICA) (14.83 ±2.4 mm). In our study, the children MMD group mean ICD at the horizontal cavernous ICA (at level of pituitary gland) was ICD 3a= 22.43 mm and at the level of petrous ICA (at IAC level) was 25.74 mm. We did not make measurements at the distal or proximal dural ring but rather used the ophthalmic artery as a landmark for the measurement of ICD 1 = 19.29 mm. Sawant N et al also found that pneumatisation and continued skull base development during childhood showed variation in ICD which were statistically different in children < 6 years and children who were 10-12 years. This was also why we analysed the adult MMD patients with controls from an adult population.

Tulika Gupta studied intercarotid distance by measuring the distance between carotid sulci on either side of the sella in a disarticulated sphenoid bone, at the anterior most point, posterior most point and at the maximum depth of the sella.(38). 34.2% of the specimens had the narrowest distance at the anterior point and 34.2 % posterior points, where as 26% patients had the narrowest point at the maximum depth of the sella. The narrowest ICD measured was 7.63 mm. The study showed that inter carotid

distance varies considerably along the cavernous segment. We measured the ICD 3a at the level of the carotid artery corresponding to the pituitary gland. However, our measurement was between the central lines as opposed to the medial wall of the carotid measured by Tulika Gupta in the above study. Although, there was a variation amongst our individual cases and controls, there was no significant difference between adult mmd and pediatric mmd and adult mmd and controls in our study at the level of the cavernous ICA. The supraclinoid ICA ICD (ICD3b) at the same level when compared was significantly different between the Adult MMD and children MMD group as well as the adult MMD group and controls (mean-19.56 vs 19.24, p= 0.008 and 19.56 vs 18.76 p= 0.03). ICD measured at the level of the ophthalmic artery was also significantly different between the 3 groups (mean- 21.093 vs 19.29, p= 0.018 and 21.093 vs 19.79, p= 0.016). Which means as postulated in the co author's 2018 paper (7), the supraclinoid ICA is a strong determining factor and not only is there a straightening in a sagittal plane, there is also splaying in the coronal plane behaving like an air dancer would to variations in turgidity and hemodynamic stress due to mechanical properties of it's wall.

ICD was studied among 19 patients with pituitary macro adenomas and age matched controls by Nunes et al (39). They measured ICD at the petrous ICA after the cranial bend (ICD 1) and cavernous ICA at the mid level of it's horizontal part (ICD 2). The mean ICD at petrous ICA was 21.18 ± 2.49 mm in cases and 19.89 ± 2.65 mm in controls and the difference was not statistically significant. We measured ICD at the petrous ICA at the level of IAC in the axial section which corroborated with the cranial bend as in the above study. The mean ICD was 26.35 mm in adult MMD cases, 25.74 in children with MMD and 25.74 in controls and there was no statistically significant difference between adult and children MMD and adult MMD and controls. The larger values were because they considered medial wall to medial wall narrowest distance between the two ICAs as opposed to measurement between the 2 respective central lines as in our study. Nunes et al also measured *'ICD 2'* which was 24.27 ± 5.14 mm for cases and 19.41 ±3 mm for controls and the difference was statistically significant. The value of *'ICD 2'* was significantly larger for patients with

giant pituitary adenomas than macro adenomas < 4 cms and controls. Thus, they concluded that a pathological process cranial to the petrous segment had directly altered the cavernous ICA morphology.

Farimaz et al found the cavernous ICD at the mid level of sella to be 15.8 ±3.8 mm in females and 17.1 ± 4.7 mm in males and the overall gender non specific mean ICD at that level was 16.5 mm(40). Some of the other studies and the ICD values have been mentioned in the table below.

	Researchers	ID in mm	No of cases
Cadver Study	Fujii 1979 (41)	17	25
	Ozcan 2010 (42)	13.33	29
	Abuzayed 2010 (43)	13.22	30
	Aktas 2013 (44)	15.33	28
	Perondi 2013 (45)	18	30
	Cebula 2014 (46)	12.15	20
MR Study	Scotti 1988 (47)	16.6	25
	Knappe 2009 (48)	17.8	117
	Zada 2011 (49)	16.2	100
	Sasagawa 2013 (50)	19.4	138
CT Angiography Study	Zhang 2012 (51)	20.6	96
	Farimaz 2019 (40)	16.5	173

Kim T et al (8) found shorter actual distance of the ICA measured from carotid canal to the carotid siphon (p=0.0170). They found that in MMD the tortuosity was significantly reduced showing '*lower curvature angles in the petrous and intra cavernous segments'*. In their methodology they used 3D TOF sequences as in our study for 3D reconstruction. The lower point was fixed at the cerebellar tonsil and the

upper point was fixed at the carotid siphon. Both these landmarks were unfavourable to us as the carotid siphon is a broad area and the cerebellar tonsils were bound to change in position depending on multiple factors. We fixed our upper point at the origin of the ophthalmic artery as the supraclinoid ICA was too narrow for 3D reconstruction in advanced MMD cases. In those cases where the ophthalmic artery was abnormal in location or absent, we did not perform tortuosity and 'BVH' measurements. We found 5 cases with no ophthalmic artery and 3 cases where the ophthalmic artery was arising from the middle meningeal artery. The lower point was set at the mid level of the mandibular head assuming bony landmarks to be more consistent than soft tissue landmarks. Centerline was used for these measurements in both the study. The linear distance (LD) was the shortest length between the upper lower points. The actual distance (AD) of the ICA was the whole length of the centerline in the same segment.

We used the formula for Tortuosity as (AD/LD -1)*100.

Unlike in our study they did not find significance for linear distance and found significance for actual distance and tortuosity. In the above mentioned study, the MMD group was significantly younger to the control group in comparison. The authors have remarked that a limitation in their study was that they were not able to arrive at whether the change in ICA morphometrics was a result of or caused ICA bifurcation narrowing. Our findings of reduced linear distance, actual distance, tortuosity and BVH irrespective of Suzuki grading tends to point at the former, i.e change in morphometrics leading to progressive narrowing of ICA bifurcation.

We decided to measure 'Base vertex height' from the Kim T et al (8) paper's statement on loss of curvature in petrous and cavernous segment. Accordingly a straight line was drawn between the upper and lower points and perpendicular distance of the apex of the curves was measured from this line. BVH 2, 3 and 4 were found to be statistically significant as compared to the controls in adult MMD patients where clearly this deviation of the curves was far smaller in the adult MMD group than the controls. The subset of vasculitis patients when compared with the

adult MMD patients for the base vertex height alone showed that the curves were of lesser altitude in the adult MMD group and the difference was statistically significant. This also shows us that unlike what was previously thought, MMD vessel pathology is not limited to the supraclinoid segment but is a generalised disease affecting the entire course of intracranial vessels. Lee et al (52) demonstrated that a smaller P1-Basilar artery angle was a risk for posterior circulation strokes in MMD.

Jittapiromsak et al (53) classified the intracavernous ICA as redundant and normal. The redundant type was where the posterior bend courses higher than horizontal segment resulting in a tortuous course. The zero and negative values for posterior bend angles in our study in both cases and controls was due to such a configuration of ICA. In their study they called the posterior bend angle ***PBA*** *as* ***ICA curve angle*** i.e at the junction of axis of horizontal and posterior vertical segment. The cavernous roof angle (CRA) was calculated in the parasaggital view of the cavernous sinus and drawing a line along the roof and another along the posterior wall and measuring their angle of convergence. They defined redundancy of the cavernous ICA as the ratio of PBA and CRA < 0.5. Redundant cavernous ICA was seen bilaterally in 18/100 patients and unilaterally in 19/100 i.e 27% of the ICAs observed were redundant. The BVH-3 line that is measured in our study essentially measures the curvature of the cavernous ICA along the posterior bend angle and was found to be significantly reduced in the Adult MMD cohort.

Yasuda et al(54) described the Champagne Bottle neck sign in **extra cranial ICA** in patients with MMD. They believed there is a rapid reduction in the size of EC-ICA in MMD but the timing of onset is not predictable . Ratio between EC-ICA and CCA was measured by angiography or neck doppler ultrasound and < 0.5 was considered champagne bottle neck sign. They also observed the ratio to be smaller in higher stages of the disease with all positive cases for the sign classified as '≥ stage 3' with decreased cerebral reactivity to acetazolamide when accessed with SPECT. We could not perform this as the TOF images that were taken did not cover cervical ICA bifurcation.

CONCLUSION

The findings of this study bring us one step closer in supporting the mechanobiological theory of MMD (6). As suggested in the hypothesis, altered craniofacial development tied to the development of intracranial vessels are probably an antecedent factor to narrowing of the ICA bifurcation and not the other way around. Reduced tortuosity with higher angles and smaller curves leads to a failure of dampening of the haemodynamic forces before the blood reaches the intracranial cavity. The higher stresses experienced by the supraclinoid ICA contribute to the pathogenesis of MMD. The other aspects discussed in the hypothesis shall be the direction of future studies to further the evidence towards solving the puzzle of pathogenesis in MMD.

LIMITATIONS

We did not find sufficient TOF images among non MMD pediatric patients in our hospital. Hence, we did not use a control group to analyse data between non MMD pediatric controls and pediatric MMD cases. Once sufficient data is available that shall be assessed in part 2 of this study.

Funding: No Funding was received for this study.

Bibliography

1. Nagaraja D, Verma A, Taly AB, Veerendra Kumar M, Jayakumar PN. Cerebrovascular disease in children. Acta Neurologica Scandinavica. 1994;90(4):251-5.
2. Soriano SG, Sethna NF, Scott RM. Anesthetic management of children with moyamoya syndrome. Anesth Analg. 1993;77(5):1066-70.
3. Baba T, Houkin K, Kuroda S. Novel epidemiological features of moyamoya disease. J Neurol Neurosurg Psychiatry. 2008;79(8):900-4.
4. Wakai K, Tamakoshi A, Ikezaki K, Fukui M, Kawamura T, Aoki R, et al. Epidemiological features of moyamoya disease in Japan: findings from a nationwide survey. Clin Neurol Neurosurg. 1997;99 Suppl 2:S1-5.
5. Scott RM, Smith JL, Robertson RL, Madsen JR, Soriano SG, Rockoff MA. Long-term outcome in children with moyamoya syndrome after cranial revascularization by pial synangiosis. J Neurosurg. 2004;100(2 Suppl Pediatrics):142-9.
6. Sudhir BJ, Keelara AG, Venkat EH, Kazumata K, Sundararaman A. The mechanobiological theory: a unifying hypothesis on the pathogenesis of moyamoya disease based on a systematic review. Neurosurg Focus. 2021;51(3):E6.
7. Sudhir BJ, K SK, editors. Moyamoya Disease: Using Computational Fluid Dynamics to Propose a Novel “Mechanical Theory” of Pathogenesis. 2018 International Conference on Intelligent Informatics and Biomedical Sciences (ICIIBMS); 2018 21-24 Oct. 2018.
8. Kim T, Bang JS, Kwon OK, Hwang G, Kim JE, Kang HS, et al. Morphology and related hemodynamics of the internal carotid arteries of moyamoya patients. Acta Neurochir (Wien). 2015;157(5):755-61.
9. Sho E, Nanjo H, Sho M, Kobayashi M, Komatsu M, Kawamura K, et al. Arterial enlargement, tortuosity, and intimal thickening in response to sequential exposure to high and low wall shear stress. J Vasc Surg. 2004;39(3):601-12.
10. Sho M, Sho E, Singh TM, Komatsu M, Sugita A, Xu C, et al. Subnormal shear stress-induced intimal thickening requires medial smooth muscle cell proliferation and migration. Exp Mol Pathol. 2002;72(2):150-60.
11. Sawant N, Sabarish S, George T, Shivhare P, Sudhir B, Kesavadas C, et al. A Study of the Developing Paediatric Skullbase Anatomy and its Application to Endoscopic Endonasal Approaches in Children. Neurology India. 2020;68(5):1065-72.
12. Suzuki J, Takaku A. Cerebrovascular "moyamoya" disease. Disease showing abnormal net-like vessels in base of brain. Arch Neurol. 1969;20(3):288-99.
13. Smith JL. Understanding and treating moyamoya disease in children. Neurosurg Focus. 2009;26(4):E4.
14. Kitahara T, Okumura K, Semba A, Yamaura A, Makino H. Genetic and immunologic analysis on moya-moya. Journal of neurology, neurosurgery, and psychiatry. 1982;45(11):1048-52.
15. Han DH, Nam DH, Oh CW. Moyamoya disease in adults: characteristics of clinical presentation and outcome after encephalo-duro-arterio-synangiosis. Clin Neurol Neurosurg. 1997;99 Suppl 2:S151-5.
16. Fujimura M, Funaki T, Houkin K, Takahashi JC, Kuroda S, Tomata Y, et al. Intrinsic development of choroidal and thalamic collaterals in hemorrhagic-onset moyamoya disease: case-control study of the Japan Adult Moyamoya Trial. Journal of Neurosurgery JNS. 2019;130(5):1453-9.
17. Miyamoto S, Kikuchi H, Karasawa J, Nagata I, Ihara I, Yamagata S. Study of the posterior circulation in moyamoya disease. Part 2: Visual disturbances and surgical treatment. J Neurosurg. 1986;65(4):454-60.
18. Srivastava T, Sannegowda RB, Mittal RS, Jain RS, Tejwani S, Jain R. An institutional experience of 26 patients with Moyamoya disease: A study from Northwest India. Ann Indian Acad Neurol. 2014;17(2):182-6.

19. Sadashiva N, Reddy YV, Arima A, Saini J, Shukla D, Pandey P. Moyamoya disease: Experience with direct and indirect revascularization in 70 patients from a nonendemic region. Neurol India. 2016;64 Suppl:S78-86.
20. Kelly ME, Bell-Stephens TE, Marks MP, Do HM, Steinberg GK. Progression of unilateral moyamoya disease: A clinical series. Cerebrovasc Dis. 2006;22(2-3):109-15.
21. Kuroda S, Houkin K. Moyamoya disease: current concepts and future perspectives. Lancet Neurol. 2008;7(11):1056-66.
22. An S, Kim T, Oh CW, Bang JS, Lee SU, Heo J. Vascular tortuosity of the internal carotid artery is related to the RNF213 c.14429G>A variant in moyamoya disease. Sci Rep. 2019;9(1):8614.
23. Zhang H, Zheng L, Feng L. Epidemiology, diagnosis and treatment of moyamoya disease. Exp Ther Med. 2019;17(3):1977-84.
24. Fukui M, Kono S, Sueishi K, Ikezaki K. Moyamoya disease. Neuropathology. 2000;20 Suppl:S61-4.
25. Menon G, Hegde A. Moyamoya disease. Archives of Medicine and Health Sciences. 2019;7(2):224-32.
26. Yamada I, Suzuki S, Matsushima Y. Moyamoya disease: comparison of assessment with MR angiography and MR imaging versus conventional angiography. Radiology. 1995;196(1):211-8.
27. Jeon JP, Kim JE, Cho WS, Bang JS, Son YJ, Oh CW. Meta-analysis of the surgical outcomes of symptomatic moyamoya disease in adults. J Neurosurg. 2018;128(3):793-9.
28. Acker G, Fekonja L, Vajkoczy P. Surgical Management of Moyamoya Disease. Stroke. 2018;49(2):476-82.
29. Sun H, Wilson C, Ozpinar A, Safavi-Abbasi S, Zhao Y, Nakaji P, et al. Perioperative Complications and Long-Term Outcomes After Bypasses in Adults with Moyamoya Disease: A Systematic Review and Meta-Analysis. World Neurosurg. 2016;92:179-88.
30. Sudhir BJ, Karthikayan A, Amjad JM, Arun KG. Strategic tunnelling of superficial temporal artery during bypass surgery for moyamoya disease. Acta Neurochir (Wien). 2022;164(4):1021-5.
31. Czabanka M, Peña-Tapia P, Scharf J, Schubert GA, Münch E, Horn P, et al. Characterization of direct and indirect cerebral revascularization for the treatment of European patients with moyamoya disease. Cerebrovasc Dis. 2011;32(4):361-9.
32. Menshawi K, Mohr JP, Gutierrez J. A Functional Perspective on the Embryology and Anatomy of the Cerebral Blood Supply. J Stroke. 2015;17(2):144-58.
33. Bouthillier A, van Loveren HR, Keller JT. Segments of the internal carotid artery: a new classification. Neurosurgery. 1996;38(3):425-32; discussion 32-3.
34. Inoue T, Rhoton AL, Jr., Theele D, Barry ME. Surgical approaches to the cavernous sinus: a microsurgical study. Neurosurgery. 1990;26(6):903-32.
35. Fedorov A, Beichel R, Kalpathy-Cramer J, Finet J, Fillion-Robin JC, Pujol S, et al. 3D Slicer as an image computing platform for the Quantitative Imaging Network. Magn Reson Imaging. 2012;30(9):1323-41.
36. Bang OY, Fujimura M, Kim S-K. The Pathophysiology of Moyamoya Disease: An Update. J Stroke. 2016;18(1):12-20.
37. Kotani Y, Morito D, Yamazaki S, Ogino K, Kawakami K, Takashima S, et al. Neuromuscular regulation in zebrafish by a large AAA+ ATPase/ubiquitin ligase, mysterin/RNF213. Scientific Reports. 2015;5(1):16161.
38. Gupta T. An anatomical study of inter carotid distances in the sellar region with a surgical perspective. Brazilian Journal for Morphological Sciences. 2009;26:23-6.
39. Nunes CF, Cabral GA, Mello Junior JO, Lapenta MA, Landeiro JA. Pituitary macroadenoma: analysis of intercarotid artery distance compared to controls. Arq Neuropsiquiatr. 2016;74(5):396-404.

40. Farımaz M, Çelik HH, Ergun KM, Akgöz A, Urfalı B. The morphometry of the cavernous part of the internal carotid artery. Folia Morphologica. 2019;78(1):54-62.
41. Fujii K, Chambers SM, Rhoton AL, Jr. Neurovascular relationships of the sphenoid sinus. A microsurgical study. J Neurosurg. 1979;50(1):31-9.
42. Ozcan T, Yilmazlar S, Aker S, Korfali E. Surgical limits in transnasal approach to opticocarotid region and planum sphenoidale: an anatomic cadaveric study. World Neurosurg. 2010;73(4):326-33.
43. Abuzayed B, Tanriover N, Gazioglu N, Ozlen F, Cetin G, Akar Z. Endoscopic anatomy and approaches of the cavernous sinus: cadaver study. Surg Radiol Anat. 2010;32(5):499-508.
44. Aktas U, Yilmazlar S, Ugras N. Anatomical restrictions in the transsphenoidal, transclival approach to the upper clival region: a cadaveric, anatomic study. J Craniomaxillofac Surg. 2013;41(6):457-67.
45. Perondi GE, Isolan GR, de Aguiar PH, Stefani MA, Falcetta EF. Endoscopic anatomy of sellar region. Pituitary. 2013;16(2):251-9.
46. Cebula H, Kurbanov A, Zimmer LA, Poczos P, Leach JL, De Battista JC, et al. Endoscopic, endonasal variability in the anatomy of the internal carotid artery. World Neurosurg. 2014;82(6):e759-64.
47. Scotti G, Yu CY, Dillon WP, Norman D, Colombo N, Newton TH, et al. MR imaging of cavernous sinus involvement by pituitary adenomas. AJR Am J Roentgenol. 1988;151(4):799-806.
48. Knappe UJ, Jaursch-Hancke C, Schönmayr R, Lörcher U. Assessment of normal perisellar anatomy in 1.5 T T2-weighted MRI and comparison with the anatomic criteria defining cavernous sinus invasion of pituitary adenomas. Cent Eur Neurosurg. 2009;70(3):130-6.
49. Zada G, Agarwalla PK, Mukundan S, Jr., Dunn I, Golby AJ, Laws ER, Jr. The neurosurgical anatomy of the sphenoid sinus and sellar floor in endoscopic transsphenoidal surgery. J Neurosurg. 2011;114(5):1319-30.
50. Sasagawa Y, Tachibana O, Doai M, Akai T, Tonami H, Iizuka H. Internal carotid arterial shift after transsphenoidal surgery in pituitary adenomas with cavernous sinus invasion. Pituitary. 2013;16(4):465-70.
51. Zhang Y, Tian Y, Song J, Li Y, Li W. Internal carotid artery in endoscopic endonasal transsphenoidal surgery. J Craniofac Surg. 2012;23(6):1866-9.
52. Lee JY, Kim SK, Cheon JE, Choi JW, Phi JH, Kim IO, et al. Posterior cerebral artery involvement in moyamoya disease: initial infarction and angle between PCA and basilar artery. Childs Nerv Syst. 2013;29(12):2263-9.
53. Jittapiromsak P, Sabuncuoglu H, Deshmukh P, McDougall CG, Spetzler RF, Preul MC. Anatomical relationships of intracavernous internal carotid artery to intracavernous neural structures. Skull Base. 2010;20(5):327-36.
54. Yasuda C, Arakawa S, Shimogawa T, Kanazawa Y, Sayama T, Haga S, et al. Clinical Significance of the Champagne Bottle Neck Sign in the Extracranial Carotid Arteries of Patients with Moyamoya Disease. AJNR Am J Neuroradiol. 2016;37(10):1898-902.

Study Proforma

Study Title: COMPARISON OF ICA MORPHOMETRY BETWEEN PATIENTS WITH MOYAMOYA DISEASE AND CONTROLS

PI/neuroradiologist

Code Number:
Age :
Gender:
Symptoms:
Duration of Symptoms:
Neurological Deficits:
Co-morbidities:

Primary (Moyamoya syndrome) or secondary (Moyamoya disease):
If secondary, diagnosis:
Unilateral or Bilateral Disease

Pre op or Post op:

If Post op
Direct or Indirect revascularisation procedure:
Days of Post op stay:
Unilateral or Bi-lateral Surgery:
Complications:
Post operative follow up:

If conservatively managed:
Follow up-

Meaurements

A) Cavernous- supraclinoid ICA angle-
B) Posterior Bend angle
C) Intercarotid distance-
- ICD1
- ICD2
- ICD 3a
- ICD 3b
- ICD 4

D)
- LD
- AD
- Tortuosity

E) BVH
- BVH-1
- BVH-2
- BVH-3
- BVH-4

The measurement will be made by the principal investigator, Neuroradiologist and vetted by the co- principal investigator to reduce errors.

QuillBot

QuillBot

Scanned on: 17:5 December 14, 2022 UTC

Results

Sources that matched your submitted document.

No results found. The content is free of plagiarism.

IDENTICAL

Identical matches are one to one exact wording in the text.

MINOR CHANGES

Nearly identical with different form, ie "slow" becomes "slowly".

Unsure about your report?

The results have been found after comparing your submitted text to online sources, open databases and the Copyleaks internal database. For any questions about the report contact us on support@copyleaks.com

Learn more about different kinds of plagiarism here

QuillBot

QuillBot

Scanned on: 17:5 December 14, 2022 UTC

Scanned Text

Your text is highlighted according to the matched content in the results above.

IDENTICAL MINOR CHANGES

Moyamoya disease is a fairly rare, non atherosclerotic ischemic disease characterized by chronic progressive intracranial terminal ICA narrowing with opening up of collaterals from lenticulostriate arteries resulting in the characteristic puff of smoke appearance on angiography. The stenosis commonly extends to the proximal MCA and ACA and rarely to PCA and basilar artery (1),(2).
The disease has a bimodal age distribution, predominantly affecting children in the first decade and another peak is seen in adults later on in life (3),(4),(5). It is the most common cause of pediatric strokes in Japan. (1)
A systematic review by B.J. Sudhir et al proposed a mechanobiological hypothesis on the pathogenesis of moyamoya disease (MMD) (6). It was observed that in MMD patients, there was a loss of tortuosity in ICA measured in terms of cavernous supraclinoid angle of ICA(7),(8). It is believed that the higher cavernous supraclinoid ICA angle exerted a higher hemodynamic stress at ICA bifurcation. This higher wall shear stress could theoretically lead to vessel wall remodelling and narrowing as in MMD. (9),(10)
Kim T et al (8) found shorter distance measured from carotid canal to the carotid siphon in addition to higher cavernous-supraclinoid ICA angles.
Inter-carotid distance (ICD) has not been measured in patients with MMD. Sawant N et al (11) measured ICD in pediatric patients with no skull base pathology and found the narrowest ICD was at the level of the proximal dural ring measuring 13.4 mm. Altered growth kinetics in MMD patients may affect tortuosity and ICD.
The outcome of this study is expected to give further credence to the mechano-biological hypothesis for pathogenesis of MMD (6). It may give clarity on whether the altered morphometrics are a cause or a result of the reduced ICA blood flow in MMD. This in turn might alter the management protocols in the future.
The motivation for the work put into this dissertation are two of the earlier papers published by the co-principal investigator. The first of which was a discussion on the effect of hemodynamic stress due to a higher cavernous-supraclinoid angle and reduced tortuosity in moyamoya disease on vascular remodelling that occurs in the same(1). In the study methodology, the angles were measured between the lines drawn through mid point of diameters of cavernous and supraclinoid segment on DSA in saggital plane. We intended to obtain the true central line for a more accurate representation using 3D slicer© technology. The mean cavernous- supraclinoid ICA angle in the above mentioned study was 69.7 degrees in MMD and 40.5 degrees in control group, the difference being statistically significant. However, in our study the mean cavernous- supraclinoid ICA angle was 38.46 degrees in adult MMD, 50 degrees in children with MMD and 31.02 degrees in controls. The difference was significant in both the studies. In the same paper, CAD model of a normal ICA was subjected to increasing cavernous supraclinoid angle and CFD analysis was carried out to arrive at the wall shear stress (WSS) at ICA bifurcation. The wall shear stress was found to be directly proportional to the cavernous supraclinoid ICA angle amongst the 4 variations measured. Kim T et al (2) in their study created two 3D models, one for MMD patients and one for control and ran CFD analysis to find a higher flow velocity and WSS at terminal ICA bifurcation and proximal ICA and MCA in the MMD ICA model. Postmortem histopathological examination of intracranial ICA belonging to deceased patients with MMD revealed fibrocellular intimal thickening at diseased areas and proliferative smooth muscle cells with no atherosclerosis / inflammation seen(3) (4). The supraclinoid ICA in MMD was postulated to have an increased mobility in the subarachnoid cisternal space ‘like an air dancer’ due to decreased vessel wall strength resulting in the fibrocellular intimal thickening going haywire(1). The increased wall shear stress combined with an abnormal vessel mobility results in a

श्री चित्रा तिरुनाल आयुर्विज्ञान और प्रौद्योगिकी संस्थान, त्रिवेन्द्रम
तिरुवनन्तपुरम - ६९५०११, केरल, इंडिया
SREE CHITRA TIRUNAL INSTITUTE FOR MEDICAL SCIENCES AND TECHNOLOGY, TRIVANDRUM
Thiruvananthapuram - 695 011, Kerala, India
(An Institute of National Importance under Govt. of India)
Grams : Chitramet, Phone : +91-471-2443152, Fax : +91-471-2550728 / 2446433, E-mail : sct@sctimst.ac.in, Website : www.sctimst.ac.in

DUPLICATE

Institutional Ethics Committee

(IEC Regn No. ECR/189/Inst/KL/2013/RR-21)

SCT/IEC/1891/MAY/2022

11.08.2022

Dr. Sanjay HM
Post Doctoral Fellow
Department of Neurosurgery
SCTIMST, Thiruvananthapuram

Dear Dr. Sanjay,

The Institutional Ethics Committee held on 13th May, 2022, reviewed and discussed your application to conduct the study titled **"COMPARISON OF ICA MORPHOMETRY BETWEEN PATIENTS WITH MOYAMOYA DISEASE AND CONTROLS"** (IEC/1891).

The following members of the Ethics Sub-committee were present at the meeting held on 13th May, 2022.

SL. No.	Member Name	Highest Degree	Gender	Scientific /Non Scientific	Affiliation with Institution(s)
1.	Dr. Pradeep S	MBBS, MD	Male	Basic Medical Scientist	No
2.	Smt. Sathi Nair	MA (English Literature)	Female	Lay Person	No
3.	Dr. Christina George	MD Psychiatry	Female	Clinician	No
4.	Dr. P. Manickam	BSMS, MSc (Epid).,PhD	Male	Health Science Expert/ Social Scientist	No
5.	Adv. Priya Kaimal	LLM, MBL	Female	Legal Expert	No
6.	Dr. Manikandan.S	MBBS,MD,PDCC	Male	Clinician	Yes
7.	Dr. Srinivas G	PhD	Male	Basic Medical Scientist (Member Secretary)	Yes

SCT/IEC/1891/MAY-2022

The following documents were reviewed:

Original submission

1. *Checklist Form*
2. *Covering letter addressed to the Chairperson, IEC, SCTIMST dated 2.3.2022*
3. *Covering letter addressed to the Chairman, IEC, SCTIMST*
4. *IEC Application Form*
5. *Declaration form*
6. *Project Proposal*
7. *Proforma*
8. *CV of PI and Co-PIs*
9. *SRC Recommendation Letter*

Revised submission

1. *Checklist Form*
2. *Covering letter addressed to the Chairperson, IEC, SCTIMST dated 2.3.2022*
3. *Covering letter addressed to the Chairman, IEC, SCTIMST*
4. *IEC Application Form*
5. *Declaration form*
6. *Project Proposal*
7. *Proforma*
8. *CV of PI and Co-PIs*

IEC Decision

The IEC approved the conduct of the study in the present form.

Remarks:
The Institutional Ethics Committee expects to be informed about the progress of the study, any SAE occurring in the course of the study, any changes in the protocol and patient information/informed consent and asks to be provided a copy of the final report.

There was no member of the study team who participated in voting / decision making process. The ethics committee is organized and operated according to the requirements of Good Clinical Practice and the requirements of the Indian Council of Medical Research (ICMR).

Sincerely,

Dr. G. Srinivas
Member Secretary, IEC